Journal of Molecular Structure 1225 (2021) 129148

Contents lists available at ScienceDirect

Journal of Molecular Structure

journal homepage: www.elsevier.com/locate/molstr

Design, synthesis, DNA binding, modeling, anticancer studies and DFT calculations of Schiff bases tethering benzothiazole-1,2,3-triazole conjugates

Meshal A. Almehmadi[a], Ateyatallah Aljuhani[a], Shaya Yahya Alraqa[a], Imran Ali[a,b], Nadjet Rezki[a], Mohamed Reda Aouad[a,*], Mohamed Hagar[c,d]

[a] Department of Chemistry, College of Science, Taibah University, Al-Madinah Al-Munawarah, 30002, Saudi Arabia
[b] Department of Chemistry, Jamia Millia Islamia (A Central University), New Delhi 110025, India
[c] Chemistry Department, College of Sciences, Yanbu, Taibah University, Yanbu 30799, Saudi Arabia
[d] Chemistry Department, Faculty of Science, Alexandria University, Alexandria 21321, Egypt

ARTICLE INFO

Article history:
Received 27 May 2020
Revised 4 August 2020
Accepted 24 August 2020
Available online 25 August 2020

Keywords:
Benzothiazole
1,2,3-triazole
Schiff bases
DFT calculations
Anticancer
DNA binding
Modeling

ABSTRACT

In an attempt to design and prepare a new library of anticancer candidates, focused thiopropargylated benzothiazole was reacted with ethyl azidoacetate and/or ethyl azidobenzoate to yield newer 1,2,3-triazole-benzothiazole conjugates bearing ester functionality through click chemistry approach. The hydrazinolysis of the obtained ester-based triazoles was also carried out to give the corresponding 1,2,3-triazole acid hydrazide derivatives as precursors for the synthesis of the focused Schiff bases by their condensation with various benzaldehyde derivatives. Spectroscopic study was investigated on the establishment of the structures of all newly synthesized Schiff bases bearing benzothiazole-1,2,3-triazole molecular conjugate. The newly designed hydrazones showed two isomers (*cis-E* and *trans-E*) with different isomeric distribution as confirmed by NMR spectral data and supported by DFT carried out in gas phase at B3LYP 6–311G (d,p) basis set. The DFT results showed that the *cis-E* isomer is the lower energy structure and this finding was illustrated in terms of the intermolecular H-bonding. These molecules were screened for anticancer activities with A549 and H1299 lung cancer cell lines. The anticancer activities ranged from 55 to 90%. DNA binding study was also carried out to see the mechanism of action and the DNA binding constants were of good value ranging from of 2.0×10^5 and 14.7×10^5 M^{-1}; indicating good interactions of the reported molecules with DNA. Finally, the modeling was confirmed and it was found that the results of modeling were in good agreement with the results of anticancer and DNA binding studies. All these finding confirmed that the reported molecules work as anticancer agents by interacting with DNA.

1. Introduction

Schiff bases are well known as tunable molecules containing azomethine linkage, and are emerging as popular class in organic and medicinal chemistry with distinctive features; showing versatile biological properties [1–6]. Owing to their wide spectrum of biological application, Schiff bases; especially the hydrazone derivatives; are considered as fascinating medicinal molecules for new drug development [7]. These have been extremely investigated by several researchers for their antimicrobial [8], antiviral [9], antimalarial [10], anti-inflammatory [11], antioxidant [12] and anticancer [13] activities. 1,2,3-Triazole derivatives are synthetically attainable and structurally myriad core; mostly obtained by 1,3-dipolar cycloaddition of organic azides and substituted alkynes [14]. This approach was used as the most popular method that stitches two or more bioactive scaffolds yielding several 1,2,3-triazole molecular hybrids with promising biological activities [15,16].

The 1,2,3-triazoles are versatile linkers and have been well known to build stable macromolecules with vast pharmaceutical properties such as antiviral [17], antidiabetic [18], anti-inflammatory [19], antidepressant [20], analgesic [21], antimicrobial [22] and anticancer [23] properties. As documented, Carboxyamidotriazole [24], Tazobactam [25], and Cifatrizine [26] were well known as clinically and commercially drugs which have 1,2,3-triazole motif in their skeletons. In addition, benzothiazole

* Corresponding author.
E-mail address: mr_aouad@yahoo.fr (M.R. Aouad).

https://doi.org/10.1016/j.molstruc.2020.129148
0022-2860/

rings by virtue of their wide spectrum of activities are useful building blocks of several recent interesting molecular hybrids with enhanced pharmacological properties [27–32]. Moreover, the benzothiazole conjoined Schiff bases were reported to produce new biologically active molecular hybrids dotted with significant chemotherapeutic properties [33–38]. In continuation of our efforts on the molecular hybridization as powerful strategy for producing novel array of bioactive compounds [39–43], the efforts are made to report herein an elegant and efficient approach to design and synthesize new Schiff bases carrying benzothiazole-1,2,3-triazole conjugates. Besides, the application of these molecules was ascertained by testing their anticancer potential because of a great demand of new anticancer drugs [44–49]. Additionally, the attempts are also made to determine the mechanism of action of these molecules by DNA binding and modeling studies. All the results are described in this article.

2. Results and discussion

2.1. Chemistry

The targeted Schiff bases (hydrazones) carrying benzothiazole-1,2,3-triazole molecular hybrids were prepared through muli-steps synthesis as depicted in Schemes 1–3. It should be noted that similar synthetic pathway has been previously adopted by Youssif et al. [50] for the synthesis of some novel Schiff bases carrying benzimidazole-1,2,3-triazole hybrid. Thus, the propargylated benzothiazole precursor **2** was synthesized according to our previously reported method [29] involving base-catalyzed (sodium methoxide) alkylation of 2-mercaptobenzothiazole (**1**) with propargyl bromide. The click ligation of the alkyne building block **2** with the azide residue of ethyl azidoacetate and/or ethyl 4-azidobenzoate, under optimized Cu(I)-assisted 1,3-dipolar cycloaddition reaction, led to the formation of the desired esters based benzothiazole-1,2,3-triazole molecular conjugate **3** and **4**. The click reaction required stirring at room temperature for 6 h, in the presence of $CuSO_4$-sodium ascorbate in aqueous DMSO, to afford excellent yields (85–87%) of 1,2,3-triazoles **3** and **4** (Scheme 1).

The hydrazinolysis of the 1,2,3-triazoles; carrying ester functionality **3** and/or **4**; was performed through their thermal treatment with hydrazine hydrate for 4 h furnishing on the formation of the targeted hydrazides **5** and **6** in 90 and 88% yield, respectively (Scheme 2).

The structures of the title benzothiazole-1,2,3-triazole-acid hydrazide conjugates **5** and **6** were deduced from their spectroscopic analysis (IR, ^{1}H-NMR and ^{13}C-NMR). Thus, the infrared spectrum of the hydrazide **6** confirmed the absence of the ester absorption bands (C=O, C–O) and the appearance of the $-NH_2$ and –NH– absorption bands of the hydrazide functionality at 3260–3370 cm^{-1}.

The presence of a hydrazide group in the structure of compound **6** has also been supported by its ^{1}H NMR spectrum, which revealed the appearance of two characteristic singlets around δ_H 4.62 and 9.95 ppm attributed to the N**H**$_2$ and N**H** groups, respectively. In addition, the ^{13}C NMR spectrum of compound **6** confirmed the disappearance of the characteristic ethyl ester carbons of its precursor **4** and the presence of a diagnostic carbonyl amide carbon signal (C=O) in the downfield area at δ_C 166.04 ppm.

We have anticipated the synthesis of a library of Schiff bases type hydrazone **7-22** *via* the condensation of the synthesized benzothiazole-1,2,3-triazole acid hydrazide conjugates **5** and/or **6** with an array of substituted benzaldehyde derivatives catalyzed with acetic acid (Scheme 3). The reaction mixture was heated in refluxing ethanol for 6-8 h to give excellent yields (85-93%) of the desired hydrazones **7-22**. The structures of all compounds and their spectra are given in Supplementary information.

It is noticeable that literature investigated the stereochemistry of hydrazones and reported to exist in a mixture of four diastereomers: *E/Z* geometrical isomerism around the azomethine linkage (–C=N) and *cis/trans* amide conformers [51,52]. The ratio of these isomers are dependent on many factors such as the nature of the solvent, their chelation ability, the electronic effect and the position of the attached substituents [53]. The structures of the title hydrazones **7-22** have been deduced using different spectroscopic techniques. As expected, their proposed structures were in accordance with the results previously reported for *N*-acyl substituted hydrazones [54–56], which were proved to exist in the *E*-configuration of the C=N bond in DMSO-d_6 solution due to steric hindrance on the imine bond (Scheme 4).

Based on previous reports that confirm existence of acyl and aroylhydrazones in polar solvents (such as DMSO solutions) up to 100% as *E*–isomers [57] and the *Z*-isomers are the minors of these products.

The preference of *cis*-form could be explained on the basis that *cis* conformation of amide functionality allows the CO and NH groups to make maximum intermolecular hydrogen bonding [58,59] as illustrated in Fig. 1.

The arylidene substituents play an important role to favor the predominance either the *cis* or *trans* forms, that's occur by affecting the strength of the intermolecular hydrogen bond of the chelated form. Where electron attracting substituent such as fluoro group lengthen both the carbonyl group and the N–H bond of amide functionality leading to more polarizable donor and acceptor atoms and thus effectively forming intermolecular hydrogen bond (HB), and hence these derivatives favor the *cis*-form.

To confirm the stability of the proposed diastereoisomers, the optimized structures were estimated by DFT calculations and were carried out in gas phase at B3LYP 6–311G (d,p) basis set. The calculations were performed for the proposed four isomers of the prepared compound **7** to predict the most stable isomer. This involved performing a geometry optimization on each isomer to determine the minimum energy structure, followed by a frequency calculation at the optimized geometry during which various thermochemical quantities are also computed, Fig. 2.

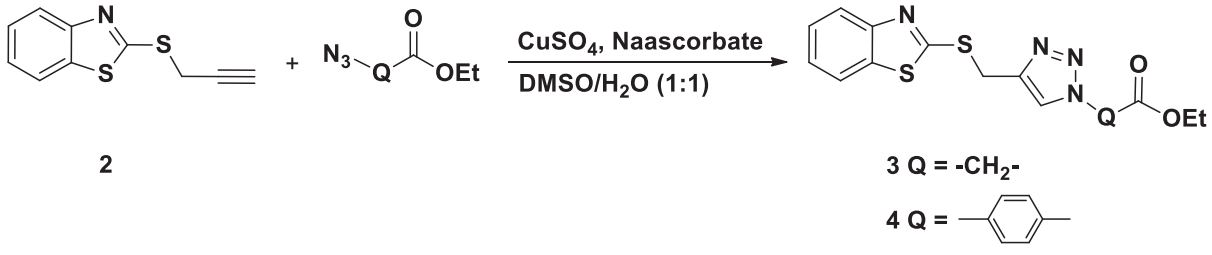

Scheme 1. Synthesis of esters based benzothiazole-1,2,3-triazole molecular conjugate **3** and **4**.

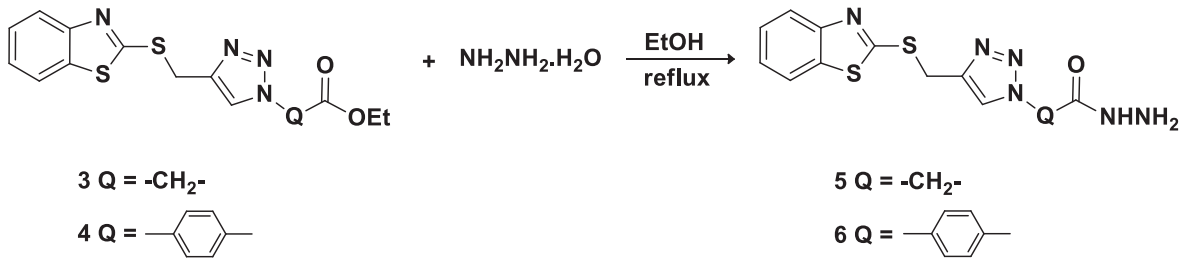

Scheme 2. Synthesis of acid hydrazides based benzothiazole-1,2,3-triazole molecular conjugate **5** and **6**.

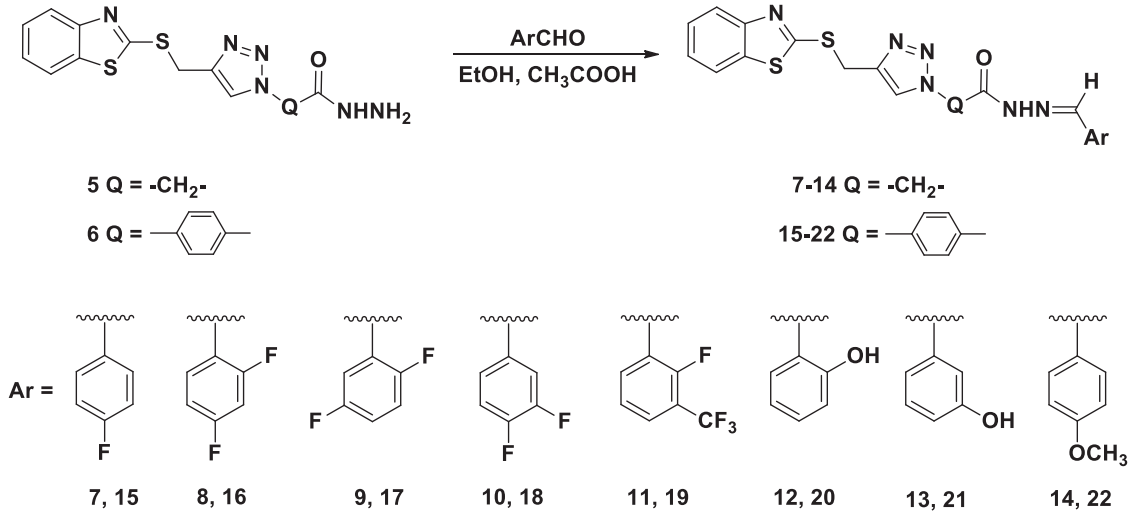

Scheme 3. Synthesis of Schiff bases (hydrazones) carrying benzothiazole-1,2,3-triazole conjugates **7-22**.

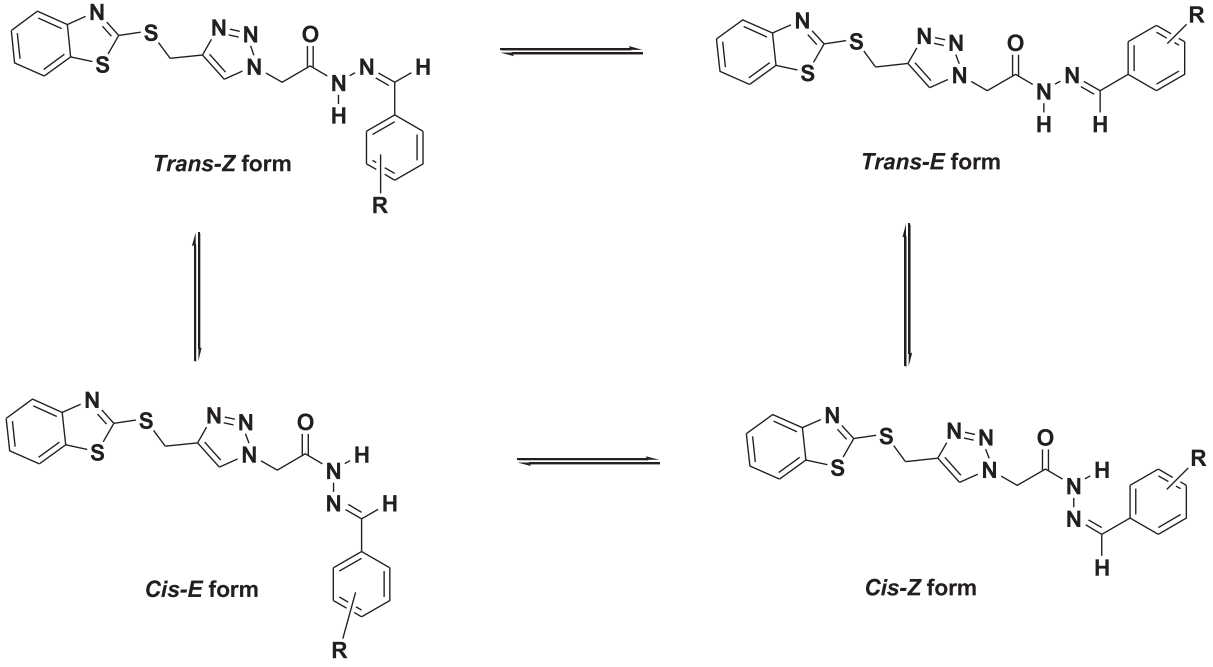

Scheme 4. Possible isomers for the prepared acylhydrazones **7-14**.

To predict the relative stabilities of the four isomeric forms for each compound, the corrected energy and the thermodynamic properties: enthalpy (H), and free energy (G) was computed, Table 1.

The results of the DFT calculations predicted that *cis-E* form is the lower energy structure and hence more stable than its isomers by 1.93, 4.8 and 7.78 Kcal/mol for *trans-E, cis-Z* and *trans-Z*, respectively. However, in DMSO showed higher difference between the proposed isomers, 2.33, 5.48 and 8.18 Kcal/mol for *trans-E, cis-Z* and *trans-Z*, respectively with respect to the *cis-E* form. It is worthy note that the DMSO solvent affects the difference of the predicted thermal energy and this could be illustrated in terms of the

Table 1
B3LYP calculated thermal-corrected energy, thermodynamic properties: enthalpy (**H**), free energy (**G**), **ΔE, ΔH, ΔG v**alues for tautomeric forms of compound **7** using 6-311G (d,p) basis set.

Parameters								
ΔG (kcal /mol)	ΔH (kcal /mol)	ΔE (kcal /mol)	G (hartrees)	H (hartrees)	E_{corr} (hartrees)	E_{tot} (hartrees)	ZPVE (hartrees)	Comp. 7
In gas phase								
Trans-Z	0.320648	-2032.536625	-2032.511440	-2032.510496	-2032.599256	7.78	7.78	8.41
Trans-E	0.320357	-2032.546027	-2032.520770	-2032.519826	-2032.608611	1.93	1.93	2.55
Cis-Z	0.320266	-2032.541500	-2032.516193	-2032.515249	-2032.604720	4.80	4.80	4.99
Cis-E	0.319938	-2032.549243	-2032.523843	-2032.522899	-2032.612677	0.00	0.00	0.00
In DMSO								
Trans-Z	0.320546	-2032.565788	-2032.540587	-2032.539642	-2032.628215	8.18	8.03	8.03
Trans-E	0.320343	-2032.575118	-2032.549813	-2032.548869	-2032.637751	2.33	2.24	2.24
Cis-Z	0.320252	-2032.570093	-2032.544732	-2032.543788	-2032.633785	5.48	5.43	5.43
Cis-E	0.319993	-2032.578841	-2032.553391	-2032.552447	-2032.643118	0.00	0.00	0.00

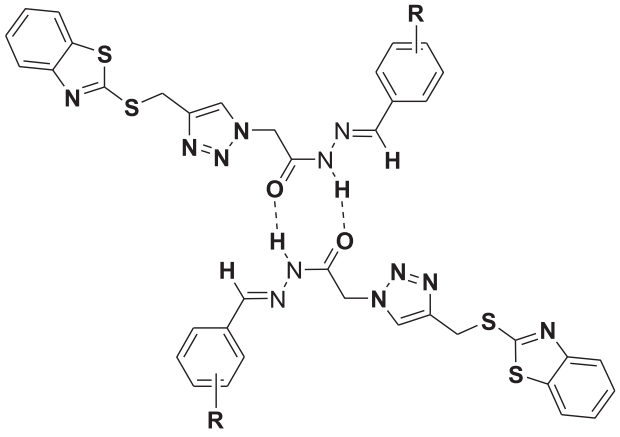

Fig. 1. The intermolecular hydrogen bond of *cis* amido form.

solvation that could give extra stability of the *cis-E* isomeric form compared to the other isomers. However, the small energy difference between the two conformations, *trans* and *cis* of the configurational *E*-isomer either in gas phase or in DMSO indicates their coexistence in equilibrium in the gas phase (Table 1).

On the other hands, the proton NMR spectra confirmed the previous results, where, it displayed the same sets of two characteristic singlets around δ_H 7.94–8.98 ppm, with a ratio varying from 1:2 to 1:9 integrating with one proton belonging to the azomethine linkage (N=C**H**). Additionally, the amide -N**H**- proton resonated also as two distinct singlets with the same ratio around δ_H 11.77-12.23 ppm. The remaining protons resonated at their appropriate chemical shifts with the same isomeric distribution to that recorded for the referred imine (–N=C**H–**) and amine (–N**H–**) protons. Moreover, the ^{13}C NMR spectra also confirmed the presence of a mixture of *trans-E* and *cis-E* diastereomers through the appearance of two sets of signals between δ_C 156.14–168.25 ppm attributed to the imine (**C**=N) and amidic carbonyl (**C**=O) carbons. Such pairing of signals were not recorded in the ^1H NMR spectra of hydrazides **5** and **6** as compared to their corresponding hydrazones **7-22**, which revealed the absence of *trans-E* and *cis-E* stereoisomerism.

However, we have deduced that Schiff bases **15-22**, derived from benzohydrazide **6**, existed as a mixture of *trans-E* and *cis-E* diastereomers in very low ratio (9:1) as compared to their analogues **7-14** (1:2, 1:3, 1:4 and 1:5) derived from acetohydrazide **5**. Consequently, it could be concluded that the difference in the isomeric pattern may result from the restricted rotation of the carbonyl amide group from *cis* conformer to *trans* conformer or *vice*

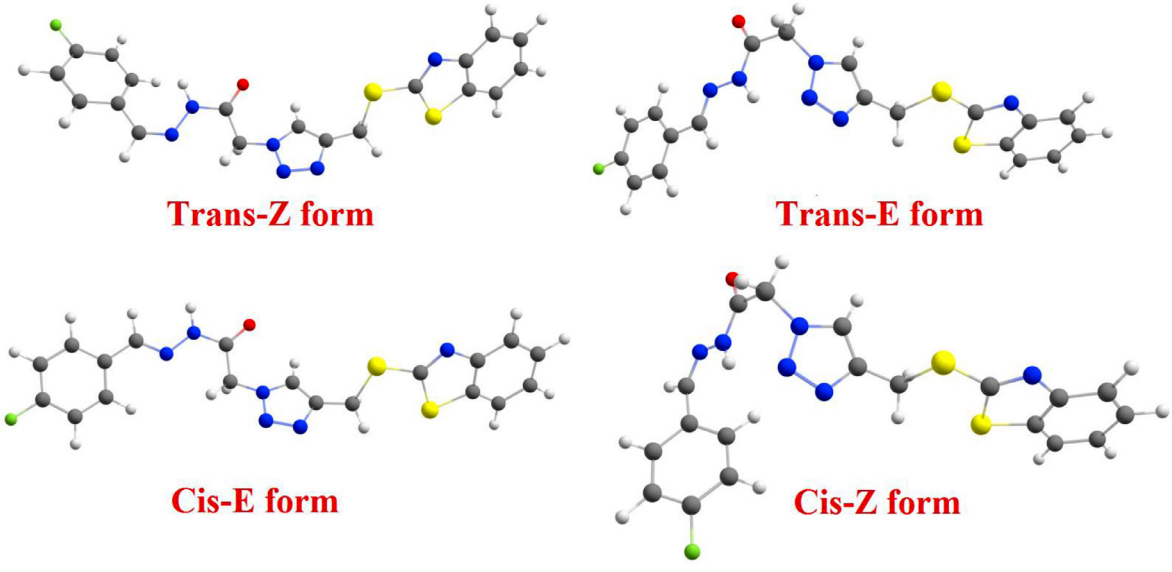

Fig. 2. Optimized molecular structure of studied isomers of compound **7**.

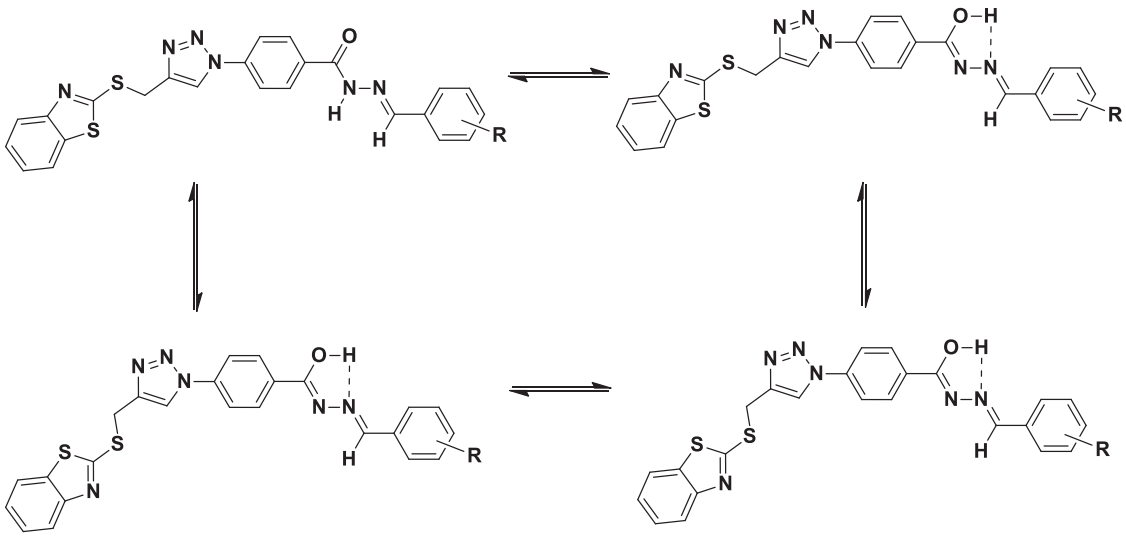

Scheme 5. Amido-amidic acid tautomerism of compounds **15-22**.

versa due to the presence of the rigid phenyl-1,2,3-triazole building block which makes this rotation very difficult.

In addition, the conjugation of the amide C=O with an aryl ring may lower the energy barrier of CO–N rotation due to competing delocalization of the C=O with the π-electrons of the aromatic ring and the non-bonding electrons of the nitrogen atom, as well as increasing the energy of the *cis* isomer with respect to the *trans* due to larger steric interactions.

Moreover, the presence of the phenyl ring in conjugation with the carbonyl group makes it more polarizable and hence increases the possibility of formation of the amidic acid form *via* amide-amidic tautomerism. Therefore, the amidic form became more predominant due to the π electrons conjugation of the phenyl ring and the carbonyl group which stabilizes the formation of the amidic acid form instead of the amido one. Moreover, the extra stability of the amidic form is also achieved by the intramolecular hydrogen bond between the (-N=N-) and NH groups in the *trans-E* isomer only. Such tendency of intramolecular hydrogen bonding confirms the formation of hydrazones **15-22** as a mixture of *trans-E* and *cis-E* isomers in 9:1 ratio, Scheme 5.

To support the formation of these Schiff bases type hydrazones, the IR and NMR spectra of compounds **12** and **18** were discussed. The IR spectrum of compound **12** showed the absence of the NH_2 absorption band and the presence of a broad absorption band around 3250-3345 cm^{-1} related to the –OH and –NH– groups.

Moreover, the ^1H NMR analysis (Fig. S21, supplementary information) also revealed the absence of the signal assigned to the hydrazide -N**H**$_2$ protons and the presence of two singlets around δ_H 7.94 and 8.11 ppm integrated for one proton, with a ratio of 1:3 belonging to the azomethine proton (–N=C**H–**). Focusing on the aliphatic protons, the -NC**H**$_2$ protons resonated also as two singlets in the up-field at δ_H 5.22 and 5.67 ppm with the same ratio. The same ratio was observed for the –N**H**– proton which appeared also as two singlets at δ_H 11.77 and 11.86 ppm. According to the literature [57], in polar aprotic solvents (DMSO-d_6) the up-field peak of methylene protons has been assigned to *trans* conformer whereas downfield peak to *cis* form. Consequently, it could be concluded that the singlets recorded at δ_H 5.65, 7.94 and 11.77 ppm are associated with the protons of the *cis* amide conformer of **12** (75%). In case of *trans-E* isomer, singlets for methylene (OC**H**$_2$), imine (-N=C**H-**) and amide (N**H**) protons were observed at δ_H 5.22, 8.11 and 11.86 ppm, respectively (25%). Additional aromatic protons were observed in their respected chemical shift attributed to the aldehyde protons.

Furthermore, the carbon NMR spectrum of Schiff base **12** (Fig. S22, supplementary information) was in accordance with the proposed structure and supported the presence of the two diastereoisomers (*trans-E* and *cis-E*). Thus, the NCH_2 carbon resonated as two signals at δ_C 51.01 and 51.42 ppm assigned to the *cis-E* and *trans-E*, respectively. The **C**=N carbons were observed as double signals at δ_C 158.09 and 162.46 ppm, while the signals recorded at δ_C 166.36 and 167.72 ppm were attributed to the **C**=O carbons. The spectrum also displayed new aromatic carbons in their respected area (See experimental section).

Similarly, the disappearance of the absorption band related to $-NH_2$ of the hydrazide group in the IR spectrum of compound **18** and the appearance of a weak –NH– band around 3254-3342 cm^{-1} confirmed the formation of the hydrazone **18**. The proton NMR analysis of Schiff base **18** (Fig. S35, supplementary information) also revealed the disappearance of the $-NH_2$ protons of the hydrazide functionality in the starting material and, thus, confirmed the success of the condensation reaction. In addition, the spectrum recorded the imine proton (–**H**C=N–) as two singlets with a 1:9 ratio at δ_H 8.44 (*cis*) and 8.97 (*trans*) ppm, respectively. The –N**H**– proton also appeared as two singlets with the same ratio at δ_H 12.01 (*cis*) and 12.13 (*trans*) ppm. Additional aromatic protons were observed attributed to the aldehydic phenyl protons.

The appearance of a mixture of *trans-E* and *cis-E* diastereoisomers for compound **18** was also evidenced by ^{13}C NMR experiment, which showed the presence of the same two sets for each signal reflecting the presence of the diastereoisomeric mixture. Thus, the carbons of the –**C**=N– and –**C**=O– groups were resonated as double peaks between δ_C 158.31–166.03 ppm (Figure S21, supplementary information). The spectral data of the newly synthesized click products **3-22** are listed in Table 2.

2.2. DNA binding study

Literature designates that around 90% anticancer drugs work by attacking cell DNA [60–67]. Consequently, the efforts were made to learn the interactions of the Schiff bases with DNA. The study of interactions of Schiff's bases with Ct-DNA was done at pH 7.4 in a solution of distilled water containing tris-(hydroxymethyl)-amino methane (Tris, 10^{-2} M). Originally, the amount of freshly prepared

Table 2
Physicochemical and NMR spectral data for the newly synthesized compounds.

Compd. No	Yield (%)	MP(°C)	MS (ESI)[M+]	IR (υ, cm^{-1})	NMR (DMSO-d_6, δ:ppm)
3	87	112-113	334.532	1555 (C=C), 1615 (C=N), 1740 (C=O), 3020 (CH-Ar)	^{1}H NMR: δ_H = 1.18 (dd, 3H, J = 4.0, 8.0 Hz, CH_3), 4.11-4.16 (q, 2H,OCH_2),4.73 (s, 2H, SCH_2), 5.36 (s, 2H, NCH_2), 7.37 (t, 1H, J = 8.0 Hz, Ar-H), 7.48 (t, 1H, J = 8.0 Hz, Ar-H), 7.91 (d, 1H, J = 8.0 Hz, Ar-H), 8.03 (d, 1H, J = 8.0 Hz, Ar-H), 8.15 (s, 1H, CH-1,2,3-triazole). ^{13}C NMR: δ_C = 14.37 (CH_3); 27.74 (SCH_2); 50.87 (NCH_2); 61.93 (OCH_2); 121.76, 122.31, 125.03, 125.85, 126.85, 135.19, 143.07, 153.06, 166.25 (Ar-C, C=N); 167.64 (C=O)
4	85	204-205	386.361	1555 (C=C), 1620 (C=N), 1730 (C=O), 3040 (CH-Ar)	^{1}H NMR: δ_H = 1.33 (t, 3H, J = 4.0 Hz, CH_3), 4.31-4.36 (q, 2H,OCH_2),4.81 (s, 2H, SCH_2), 7.37 (t, 1H, J = 8.0 Hz, Ar-H), 7.49 (dd, 1H, J = 4.0, 8.0 Hz, Ar-H), 7.93 (d, 1H, J = 8.0 Hz, Ar-H), 8.02 (d, 1H, J = 8 Hz, Ar-H), 8.05-8.13 (m, 4H, J = 8 Hz, Ar-H), 8.97 (s, 1H, CH-1,2,3-triazole). ^{13}C NMR: δ_C = 14.59 (CH_3); 27.69 (SCH_2); 61.57 (OCH_2); 119.79, 120.34, 121.78, 122.34, 122.72, 125.05, 126.88, 130.09, 131.38, 135.21, 140.05, 144.61, 153.03, 165.26 (Ar-C, C=N); 166.00 (C=O).
5	90	177-178	320.496	1565 (C=C), 1610 (C=N), 1710 (C=O), 3040 (CH-Ar), 3250-3385 (NH, NH_2)	^{1}H NMR: δ_H = 4.30 (bs, 2H,NH_2), 4.71 (s, 2H, SCH_2), 5.01 (s, 2H, NCH_2), 7.38 (t, 1H, J = 8.0 Hz, Ar-H), 7.49 (t, 1H, J = 8.0 Hz, Ar-H), 7.91 (d, 1H, J = 8.0 Hz, Ar-H), 8.02 (d, 1H, J = 8 Hz, Ar-H), 8.10 (s, 1H, CH-1,2,3-triazole), 9.53 (s, 1H, CONH). ^{13}C NMR: δ_C = 27.78 (SCH_2); 50.92 (NCH_2); 121.73, 122.33, 125.03, 126.87, 135.18, 142.58, 153.06 (Ar-C, C=N); 166.35 (C=O).
6	88	248-249	382.574	1560 (C=C), 1605 (C=N), 1705 (C=O), 3065 (CH-Ar), 3260-3370 (NH, NH_2)	^{1}H NMR: δ_H = 4.62 (bs, 2H, NH_2), 4.80 (s, 2H, SCH_2), 7.37 (t, 1H, J = 8.0 Hz, Ar-H), 7.48 (t, 1H, J = 8.0 Hz, Ar-H), 7.94 (d, 1H, J = 8.0 Hz, Ar-H), 8.00-8.04 (m, 5H,Ar-H), 8.92 (s, 1H, CH-1,2,3-triazole), 9.95 (s, 1H, CONH). ^{13}C NMR: δ_C = 27.78 (SCH_2); 50.92 (NCH_2); 121.73, 122.33, 125.03, 126.87, 135.18, 142.58, 153.06 (Ar-C, C=N); 166.35 (C=O).27.72 (SCH_2); 120.14, 121.77, 122.34, 122.65, 125.06, 126.88, 129.13, 135.20, 138.60, 144.40, 153.03 (Ar-C, C=N); 166.04 (C=O).
7	92	191-192	426.611	1605 (C=N), 1705 (C=O), 3055 (CH-Ar), 3265 (NH)	^{1}H NMR: δ_H = 4.74 (s, 2H, SCH_2), 5.22 (s, 0.5H, NCH_2, *trans*), 5.72 (s, 1.5H, NCH_2, *cis*), 7.26-7.30 (m, 2H, Ar-H), 7.38 (t, 1H, J = 8.0 Hz, Ar-H), 7.48 (t, 1H, J = 8.0 Hz, Ar-H), 7.78-7.82 (m, 2H, Ar-H), 7.92 (d, 1H, J = 8.0 Hz, Ar-H), 8.00-8.04 (m, 1.75H, HC=N, *cis* and Ar-H), 8.14 (s, 1H, CH-1,2,3-triazole), 8.21 (s, 0.25H, HC=N, *trans*), 11.84 (s, 0.75H, NH, *cis*), 11.92 (s, 0.25H, NH, *trans*). ^{13}C NMR: δ_C = 27.85 (SCH_2); 51.09 (NCH_2); 116.46, 121.75, 122.31, 125.01, 126.18, 126.85, 130.95, 135.19, 142.53, 143.72, 153.07, 162.31, 164.84, 166.35, 167.86 (Ar-C, C=N, C=O). ^{19}F NMR: δ_F = -110.53 to -110.47 and -110.25 to -110.19 (2m, 1F, Ar-F).
8	90	175-176	444.509	1615 (C=N), 1700 (C=O), 3080 (CH-Ar), 3280 (NH)	^{1}H NMR: δ_H = 4.74 (s, 2H, SCH_2), 5.24 (s, 0.4H, NCH_2, *trans*), 5.68 (s, 1.6H, NCH_2, *cis*), 7.19 (t, 1H, J = 8.0 Hz, Ar-H), 7.34-7.39 (m, 2H, Ar-H), 7.48 (t, 1H, J = 8.0 Hz, Ar-H), 7.91 (d, 1H, J = 8.0 Hz, Ar-H), 8.01-8.06 (m, 2H, Ar-H), 8.14 (s, 0.8H, HC=N, *cis*), 8.17 (s, 1H, CH-1,2,3-triazole), 8.37 (s, 0.2H, HC=N, *trans*), 11.93 (s, 0.8H, NH, *cis*), 12.06 (s, 0.2H, NH, *trans*). ^{13}C NMR: δ_C = 27.84 (SCH_2); 51.07 (NCH_2); 104.98, 109.27, 121.76, 122.32, 125.02, 126.18, 126.86, 135.19, 136.64, 142.37, 153.03, 157.04, 160.18, 166.60, 167.97 (Ar-C, C=N, C=O). ^{19}F NMR: δ_F = -116.89 to -116.82 and 116.55 to -116.48 (2m, 1F, Ar-F), -106.71 to -106.65 and -106.39 to -106.33 (2m, 1F, Ar-F).
9	88	151-152	444.698	1620 (C=N), 1695 (C=O), 3055 (CH-Ar), 3295 (NH)	^{1}H NMR: δ_H = 4.74 (s, 2H, SCH_2), 5.26 (s, 0.3H, NCH_2, *trans*), 5.72 (s, 1.7H, NCH_2, *cis*), 7.34-7.39 (m, 3H, Ar-H), 7.46-7.55 (m, 1.15H, Ar-H), 7.78-7.83 (m, 0.85H, Ar-H), 7.92 (d, 1H, J = 8.0 Hz, Ar-H), 8.03 (d, 1H, J = 8.0 Hz, Ar-H), 8.14 (s, 0.85H, HC=N, *cis*), 8.17 (s, 1H, CH-1,2,3-triazole), 8.39 (s, 0.15H, HC=N, *trans*), 12.02 (s, 0.85H, NH, *cis*), 12.16 (s, 0.15H, NH, *trans*). ^{13}C NMR: δ_C = 27.84 (SCH_2); 51.17 (NCH_2); 110.73, 112.53, 119.21, 121.75, 122.30, 123.72, 125.01, 126.16, 126.84, 135.19, 136.52, 142.58, 153.07, 156.14, 157.70, 158.59, 160.08, 166.33, 168.25 (Ar-C, C=N, C=O). ^{19}F NMR: δ_F = -126.42 to -126.32 and -125.84 to -125.72 (2m, 1F, Ar-F), -117.81 to -117.70 and -117.65 to -117.57 (2m, 1F, Ar-F).
10	86	140-142	444.225	1615 (C=N), 1690 (C=O), 3060 (CH-Ar), 3370 (NH)	^{1}H NMR: δ_H = 4.74 (s, 2H, SCH_2), 5.24 (s, 0.4H, NCH_2, *trans*), 5.70 (s, 1.6H, NCH_2, *cis*), 7.39 (dd, 1H, J = 4.0, 8.0 Hz, Ar-H), 7.46-7.58 (m, 3H, Ar-H), 7.73-7.78 (m, 0.2H, Ar-H), 7.86-7.91 (m, 1.8H,Ar-H), 8.00 (s, 0.8H, HC=N, *cis*), 8.03 (d, 1H, J = 8.0 Hz, Ar-H), 8.14 (s, 0.8H, CH-1,2,3-triazole), 8.17 (s, 0.2H, CH-1,2,3-triazole), 8.20 (s, 0.2H, HC=N, *trans*), 11.94 (s, 0.8H, NH, *cis*), 12.06 (s, 0.2H, NH, *trans*). ^{13}C NMR: δ_C = 27.73 (SCH_2); 116.01, 118.69, 120.19, 121.77, 122.34, 122.72, 124.90, 125.06, 126.88, 129.95, 132.53, 133.42, 135.21, 139.14, 144.52, 146.35, 153.04, 160.32, 165.29, 166.34, 168.11 (Ar-C, C=N, C=O). ^{19}F NMR: δ_F = -137.83 to -137.75 (m, 1F, Ar-F), -136.33 to -136.24 and -135.91 to -135.86 (2m, 1F, Ar-F).

(*continued on next page*)

Table 2 (*continued*)

Compd. No	Yield (%)	MP(°C)	MS (ESI)[M+]	IR (υ, cm^{-1})	NMR (DMSO-d_6, δ:ppm)
11	85	170-171	494.577	1605 (C=N), 1695 (C=O), 3045 (CH-Ar), 3365 (NH)	^{1}H NMR: δ_H = 4.74 (s, 2H, SCH_2), 5.27 (s, 0.4H, NCH_2, *trans*), 5.71 (s, 1.6H, NCH_2, *cis*), 7.39 (dd, 1H, *J* = 4.0, 8.0 Hz, Ar-H), 7.48 (t, 2H, *J* = 8.0 Hz,Ar-H), 7.85 (t, 1H, *J* = 8.0 Hz, Ar-H), 7.92 (d, 1H, *J* = 8.0 Hz, Ar-H), 8.03 (d, 1H, *J* = 4.0 Hz, Ar-H), 8.15-8.32 (m, 2.8H,CH-1,2,3-triazole, Ar-H and HC=N, *cis*), 8.45 (s, 0.2H, HC=N, *trans*), 12.07 (s, 0.8H, NH, *cis*), 12.23 (s, 0.2H, NH, *trans*). ^{13}C NMR: δ_C = 27.81 (SCH_2); 51.09 (NCH_2); 121.75, 122.31, 124.38, 125.01, 125.79, 126.18, 126.85, 129.02, 131.81, 135.19, 136.18, 142.62, 153.07, 157.85, 162.03, 166.34, 168.17 (Ar-C, C=N, C=O). ^{19}F NMR: δ_F = -124.45 to -124.33 and -124.11 to -123.99 (2m, 1F, Ar-F), -60.03 (d, 3F, CF_3).
12	90	222-223	424.604	1610 (C=N), 1715 (C=O), 3070 (CH-Ar), 3250-3345 (NH, OH)	^{1}H NMR: δ_H = 4.74 (s, 2H, SCH_2), 5.22 (s, 0.5H, NCH_2, *trans*), 5.65 (s, 1.5H, NCH_2, *cis*), 6.80-6.84 (m, 1H, Ar-H), 7.07-7.25 (m, 3H, Ar-H), 7.35-7.39 (m, 1H, Ar-H), 7.46-7.49 (m, 1H, Ar-H), 7.91 (d, 1H, *J* = 4.0 Hz, Ar-H), 7.94 (s, 0.75H, HC=N, *cis*), 8.03 (d, 1H, *J* = 8.0 Hz, Ar-H), 8.11 (s, 0.25H, HC=N, *trans*), 8.17 (bs, 1H, CH-1,2,3-triazole), 9.67 (s, 1H, OH), 11.77 (s, 0.75H, NH, *cis*), 11.86 (s, 0.25H, NH, *trans*). ^{13}C NMR: δ_C = 27.87 (SCH_2); 51.01, 51.42 (NCH_2); 113.05, 113.31, 117.88, 118.94, 119.50, 121.75, 122.31, 125.02, 126.85, 130.38, 135.19, 135.51, 145.10, 148.37, 153.06, 158.09, 162.46, 166.36, 167.72 (Ar-C, C=N, C=O).
13	88	204-205	424.566	1615 (C=N), 1710 (C=O), 3035 (CH-Ar), 3265-3380 (NH, OH)	^{1}H NMR: δ_H = 4.74 (s, 2H, SCH_2), 5.25 (s, 0.66H, NCH_2, *trans*), 5.65 (s, 1.34H, NCH_2, *cis*), 6.83-6.92 (m, 2H, Ar-H), 7.22-7.31 (m, 1H,Ar-H), 7.36-7.39 (m, 1H,Ar-H), 7.48 (t, 1H, *J* = 8.0 Hz, Ar-H), 7.58 (d, 0.33H, *J* = 8.0 Hz, Ar-H), 7.76 (d, 0.66H, *J* = 8.0 Hz, Ar-H), 7.92 (d, 1H, *J* = 8.0 Hz, Ar-H), 8.03 (d, 1H, *J* = 8.0 Hz, Ar-H), 8.15 (s, 0.66H, CH-1,2,3-triazole), 8.19 (s, 0.33H, CH-1,2,3-triazole), 8.34 (s, 0.66H, HC=N, *cis*), 8.44 (s, 0.33H, HC=N, *trans*), 10.08 (s, 0.66H, OH), 10.87 (s, 0.33H, OH), 11.74 (s, 0.66H, NH, *cis*), 12.11 (s, 0.33H, NH, *trans*). ^{13}C NMR: δ_C = 27.89 (SCH_2); 51.08, 51.30 (NCH_2); 116.59, 116.77, 119.88, 120.45, 121.79, 122.32, 125.02, 126.66, 126.85, 129.41, 131.86, 132.15, 135.20, 142.02, 148.00, 153.07, 153.07, 156.89, 162.53, 166.38, 167.52 (Ar-C, C=N, C=O).
14	90	199-201	438.498	1610 (C=N), 1700 (C=O), 3070 (CH-Ar), 3320 (NH)	^{1}H NMR: δ_H = 3.79 (s, 3H, OCH_3), 4.74 (s, 2H, SCH_2), 5.20 (s, 0.5H, NCH_2, *trans*), 5.64 (s, 1.5H, NCH_2, *cis*), 7.00 (d, 2H, *J* = 8.0 Hz, Ar-H), 7.38 (t, 1H, *J* = 8.0 Hz, Ar-H), 7.48 (t, 1H, *J* = 8.0 Hz, Ar-H), 7.64-7.68 (m, 2H, Ar-H), 7.92 (d, 1H, *J* = 8.0 Hz, Ar-H), 7.97 (s, 0.75H, HC=N, *cis*), 8.04 (d, 1H, *J* = 8.0 Hz, Ar-H), 8.14 (s, 1H, CH-1,2,3-triazole), 8.16 (s, 0.25H, HC=N, *trans*), 11.70 (s, 0.75H, NH, *cis*), 11.78 (s, 0.25H, NH, *trans*). ^{13}C NMR: δ_C = 27.85 (SCH_2); 51.06, 55.77 (NCH_2); 114.76, 121.75, 122.31, 125.01, 126.20, 126.86, 129.10, 129.32, 135.19, 142.49, 144.75, 153.07, 160.53, 161.28, 166.36, 167.55 (Ar-C, C=N, C=O).
15	85	231-233	488.478	1615 (C=N), 1710 (C=O), 3135 (CH-Ar), 3310 (NH)	^{1}H NMR: δ_H = 4.73 (s, 0.2H, SCH_2, *cis*), 4.82 (s, 1.8H, SCH_2, *trans*), 7.31-7.39 (m, 3H, Ar-H), 7.50 (dd, 1H, *J* = 4.0, 8.0 Hz, Ar-H), 7.81 (bs, 2H, Ar-H), 7.95 (d, 1H, *J* = 8.0 Hz, Ar-H), 8.04 (d, 1H, *J* = 8.0 Hz, Ar-H), 8.08-8.12 (m, 4H, Ar-H), 8.47 (s, 0.9H, HC=N, *trans*), 8.88 (s, 0.1H, HC=N, *cis*), 8.97 (s, 1H, CH-1,2,3-triazole), 11.90 (s, 0.1H, NH, *cis*), 12.02 (s, 0.9H, NH, *trans*). ^{13}C NMR: δ_C = 27.73 (SCH_2); 116.54, 120.21, 121.78, 122.36, 122.73, 125.07, 126.90, 129.78, 129.91, 131.38, 133.65, 135.21, 139.08, 144.51, 147.51, 153.04, 157.15, 162.43, 164.94, 166.04 (Ar-C, C=N, C=O). ^{19}F NMR: δ_F = -109.72 to -109.64 and -109.20 to -109.12 (2m, 1F, Ar-F).
16	88	223-225	506.459	1600 (C=N), 1725 (C=O), 3090 (CH-Ar), 3350 (NH)	^{1}H NMR: δ_H = 4.75 (s, 0.2H, SCH_2, *cis*), 4.82 (s, 1.8H, SCH_2, *trans*), 7.23 (t, 1H, *J* = 8.0 Hz, Ar-H), 7.36-7.40 (m, 2H, Ar-H), 7.50 (dd, 1H, *J* = 4.0, 8.0 Hz, Ar-H), 7.95 (d, 1H, *J* = 8.0 Hz, Ar-H), 8.00-8.04 (m, 2H, Ar-H), 8.08-8.14 (m, 4H, Ar-H), 8.66 (s, 0.9H, HC=N, *trans*), 8.86 (s, 0.1H, HC=N, *cis*), 8.97 (s, 1H, CH-1,2,3-triazole), 12.00 (s, 0.1H, NH, *cis*), 12.13 (s, 0.9H, NH, *trans*). ^{13}C NMR: δ_C = 27.71 (SCH_2); 116.01, 120.25, 121.78, 122.36, 122.73, 125.08, 126.90, 129.93, 135.21, 153.04, 156.52, 162.41, 165.12, 166.04 (Ar-C, C=N, C=O). ^{19}F NMR: δ_F = -116.84 to -116.77 and -116.69 to -116.63 (2m, 1F, Ar-F), -107.00 to -106.93 and -106.60 to -106.54 (2m, 1F, Ar-F).
17	87	253-255	506.672	1625 (C=N), 1705 (C=O), 3080 (CH-Ar), 3330 (NH)	^{1}H NMR: δ_H = 4.72 (s, 0.2H, SCH_2, *cis*), 4.82 (s, 1.8H, SCH_2, *trans*), 7.37-7.39 (m, 3H, Ar-H), 7.48 (t, 1H, *J* = 8.0 Hz, Ar-H), 7.64 (bs, 1H, Ar-H), 7.94 (d, 1H, *J* = 8.0 Hz, Ar-H), 8.03 (d, 1H, *J* = 8.0 Hz, Ar-H), 8.08-8.14 (m, 4H, Ar-H), 8.67 (s, 0.9H, HC=N, *trans*), 8.86 (s, 0.1H, HC=N, cis), 8.98 (s, 1H, CH-1,2,3-triazole), 12.09 (s, 0.1H, NH, *cis*), 12.21 (s, 0.9H, NH, *trans*). ^{13}C NMR: δ_C = 27.73 (SCH_2); 112.31, 118.31, 118.70, 120.25, 121.78, 122.36, 122.74, 123.92, 125.07, 126.89, 129.97, 133.22, 135.22, 139.24, 140.30, 144.55, 153.04, 157.60, 160.03, 162.48, 166.03 (Ar-C, C=N, C=O). ^{19}F NMR: δ_F = -126.14 to -126.08 and -125.99 to -125.93 (2m, 1F, Ar-F), -117.67 to -117.61 and -117.52 to -117.45 (2m, 1F, Ar-F).

(*continued on next page*)

Table 2 (*continued*)

Compd. No	Yield (%)	MP(°C)	MS (ESI)[M+]	IR (υ, cm^{-1})	NMR (DMSO-d_6, δ:ppm)
18	92	179-180	506.634	1600 (C=N), 1695 (C=O), 3035 (CH-Ar), 3280 (NH)	^{1}H NMR: δ_H = 4.73 (s, 0.2H, SCH_2, *cis*), 4.82 (s, 1.8H, SCH_2, *trans*), 7.35-7.39 (m, 1H, Ar-H), 7.48 (t, 1H, *J* = 8.0 Hz, Ar-H), 7.53-7.62 (m, 2H, Ar-H), 7.79 (t, 1H, *J* = 8.0 Hz, Ar-H), 7.94 (d, 1H, *J* = 8.0 Hz, Ar-H), 8.03 (d, 1H, *J* = 8.0 Hz, Ar-H), 8.07-8.12 (m, 4H, Ar-H), 8.44 (s, 0.9H, HC=N, *trans*), 8.86 (s, 0.1H, HC=N, *cis*), 8.97 (s, 1H, CH-1,2,3-triazole), 12.01 (s, 0.1H, NH, *cis*), 12.13 (s, 0.9H, NH, *trans*). ^{13}C NMR: δ_C = 27.73 (SCH_2); 115.83, 116.01, 118.69, 120.19, 121.77, 122.34, 122.72, 124.90, 125.06, 126.88, 129.95, 132.53, 133.42, 135.21, 139.14, 144.52, 146.35, 153.04, 158.31, 162.52, 162.82, 166.03 (Ar-C, C=N, C=O). ^{19}F NMR: δ_F = -137.75 to -137.83 (m, 1F, Ar-F), -136.33 to -136.24 and -135.86 to -135.91 (2m, 1F, Ar-F).
19	91	242-244	556.443	1605 (C=N), 1695 (C=O), 3080 (CH-Ar), 3250 (NH)	^{1}H NMR: δ_H = 4.13 (s, 0.2H, SCH_2, *cis*), 4.82 (s, 1.8H, SCH_2, *trans*), 7.37 (t, 1H, *J* = 8.0 Hz, Ar-H), 7.46-7.51 (m, 2H, Ar-H), 7.88 (dd, 1H, *J* = 4.0, 8.0 Hz, Ar-H), 7.94 (d, 1H, *J* = 8.0 Hz, Ar-H), 8.03 (d, 1H, *J* = 8.0 Hz, Ar-H), 8.08-8.13 (m, 4H, Ar-H), 8.26 (t, 1H, *J* = 8.0 Hz, Ar-H), 8.73 (s, 0.9H, HC=N, *trans*), 8.85 (s, 0.1H, HC=N, *cis*), 8.98 (s, 1H, CH-1,2,3-triazole), 12.13 (s, 0.1H, NH, *cis*), 12.28 (s, 0.9H, NH, *trans*). ^{13}C NMR: δ_C = 27.72 (SCH_2); 120.06, 121.59, 121.77, 122.34, 122.72, 124.08, 124.30, 125.06, 125.85, 126.88, 129.07, 129.99, 131.14,133.14, 135.21, 139.25, 139.67, 144.52, 153.04, 156.50, 159.07, 162.53,166.02 (Ar-C, C=N, C=O). ^{19}F NMR: δ_F = -124.58 to -124.45 (m, 1F, Ar-F), -60.03 (d, 3F, CF_3).
20	89	246-247	486.876	1615 (C=N), 1700 (C=O), 3050 (CH-Ar), 3270-3365 (NH, OH).	^{1}H NMR: δ_H = 4.73 (s, 0.2H, SCH, *cis*), 4.82 (s, 1.8H, SCH_2, *trans*), 7.37 (t, 1H, *J* = 8.0 Hz, Ar-H), 7.48 (t, 1H, *J* = 8.0 Hz, Ar-H), 7.53-7.61 (m, 2H, Ar-H), 7.81 (dd, 1H, *J* = 4.0, 8.0 Hz, Ar-H), 7.94 (d, 1H, *J* = 8.0 Hz, Ar-H), 8.03 (d, 1H, *J* = 8.0 Hz, Ar-H), 8.08-8.14 (m, 5H, *J* = 8.0 Hz, Ar-H), 8.44 (s, 0.9H, HC=N, *trans*), 8.88 (s, 0.1H, HC=N, *cis*), 8.97 (s, 1H, CH-1,2,3-triazole), 9.60 (bs, 1H, OH), 12.01 (s, 0.1H, NH, *cis*), 12.13 (s, 0.9H, NH, *trans*). ^{13}C NMR: δ_C = 27.73 (SCH_2); 112.07, 112.30, 118.56, 120.25, 121.78, 122.35, 122.74, 125.07, 126.89, 129.97, 133.20, 135.22, 139.24, 140.31, 144.55, 153.04, 156.26, 157.63, 160.03, 162.48, 166.03 (Ar-C, C=N, C=O).
21	87	235-237	486.771	1610 (C=N), 1695 (C=O), 3085 (CH-Ar), 3190-3340 (NH, OH)	^{1}H NMR: δ_H = 4.00 (s, 0.1H, SCH_2, *cis*), 4.14 (s, 0.4H, SCH_2, *cis*), 4.83 (s, 1.5H, SCH_2, *trans*), 6.84-6.88 (m, 1H, Ar-H), 7.12 (d, 1H, *J* = 4.0 Hz, Ar-H), 7.22-7.29 (m, 2H, Ar-H), 7.38 (t, 1H, *J* = 8.0 Hz, Ar-H), 7.49 (t, 1H, *J* = 8.0 Hz, Ar-H), 7.95 (d, 1H, *J* = 8.0 Hz, Ar-H), 8.04 (d, 1H, *J* = 8.0 Hz, Ar-H), 8.08-8.14 (m, 4H, Ar-H), 8.38 (s, 0.9H, HC=N, *trans*), 8.87 (s, 0.1H, HC=N, *cis*), 8.90 (s, 0.1H, CH-1,2,3-triazole), 8.98 (s, 0.1H, CH-1,2,3-triazole), 9.59 (s, 0.1H, OH), 9.68 (s, 0.9H, OH), 11.83 (s, 0.1H, NH, *cis*), 11.95 (s, 0.9H, NH, *trans*). ^{13}C NMR: δ_C = 27.73 (SCH_2); 113.08, 117.99, 119.39, 120.20, 121.79, 122.37, 122.73, 125.08, 126.90, 127.01, 129.90, 130.41, 133.54, 135.21, 135.96, 139.09, 142.78, 144.51, 148.73, 153.04, 158.15, 162.37, 162.73, 166.04 (Ar-C, C=N, C=O).
22	85	251-253	500.631	1605 (C=N), 1710 (C=O), 3070 (CH-Ar), 3275 (NH)	^{1}H NMR: δ_H = 3.81 (s, 3H, OCH_3), 4.14 (s, 0.3H, SCH_2, *cis*), 4.82 (s, 1.7H, SCH_2, *trans*), 7.00-7.04 (m, 2H, Ar-H), 7.39 (dd, 1H, *J* = 4.0, 8.0 Hz, Ar-H), 7.48 (t, 1H, *J* = 8.0 Hz, Ar-H), 7.70 (d, 2H, *J* = 8.0 Hz, Ar-H), 7.95 (d, 1H, *J* = 8.0 Hz, Ar-H), 8.03 (d, 1H, *J* = 8 Hz, Ar-H), 8.06-8.10 (m, 4H, Ar-H), 8.41 (s, 0.9H, HC=N, *trans*), 8.85 (s, 0.1H, HC=N, *cis*), 8.87 (s, 0.1H, CH-1,2,3-triazole), 8.97 (s, 0.9H, CH-1,2,3-triazole), 11.78 (s, 0.1H, NH, *cis*), 11.88 (s, 0.9H, NH, *trans*). ^{13}C NMR: δ_C = 27.73 (SCH_2); 55.77 (OCH_3); 114.83, 120.18, 121.78, 122.35, 122.72, 125.07, 126.90, 127.21, 129.27, 129.84, 133.78, 135.21, 138.98, 144.49, 148.55, 153.04, 161.39, 161.60, 162.24, 166.04 (Ar-C, C=N, C=O).

Ct-DNA solution was ascertained by UV–Vis absorption spectrometer at 260 nm wavelength (ε = 6600 M^{-1} cm^{-1}) [68]. The clarity of DNA as a stock solution of Ct-DNA was ascertained by aratio of $A_{260}/A_{280} \geq 1.80$, which shows the adequately protein-free nature of DNA [69]. The amount of the stock solution of DNA was experimentally determined by utilizing ε=6600 M^{-1} cm^{-1} at 260 nm. The additional solutions of DNA were made from a stock solution (1.6×10^{-4} M) with a fixed concentrated solution of Schiff's bases (0.01 mg/mL). To carry binding experiments, the absorption spectra of freshly Schiff's bases at a fixed concentration of (0.01 mg/mL) were taken with the increase concentration of DNA (1.1×10^{-5} to 1.5×10^{-4} M). First of all, λ_{max} and absorbance of pure DNA and compounds were recorded in tris-buffer solutions. Then, λ_{max} and absorbance of mixture *i.e.* 2.0 mL of each solution of DNA and compounds were recorded. The absorption spectra were recorded after each addition of the different concentrations of DNA solution (2.0 mL). The titration experiments were repeated five times (n = 5). The intrinsic binding constants (K_b) were determined by Benssi-Hilderbrand equation modified by Wolfe et *al.* [70]. The DNA binding constant results are shown in Table 3 while the DNA binding spectra of the most active compounds of series A (**8**) and B (**18**) are shown in Fig. 3. The spectra of rest compounds are given in Supplementary information. It is important to mention here that these drugs formed adducts with DNA; leading to deactivation of DNA activities. This remark is very significant and valuable to clarify how these molecules are control cancer. The values of DNA binding constants for these drugs were in the range of 2.0×10^5 and 14.7×10^5 M^{-1}; indicating good interactions with DNA. The max-

Table 3
Wavelength shifts, % hypochromism and binding constants.

Compd. No	λ_{max} (free)	λ_{max} (bound to DNA)	Change in λ_{max}	% Hypochromism[a]	K_b (M^{-1})
3	223nm	223nm	0	39.11	4.76×10^5
4	271nm	267nm	3	33.96	4.3×10^5
5	223nm	223nm	0	40.13	5.7×10^5
6	270nm	266nm	4	17.56	6.0×10^5
7	223nm	271nm	48	26.79	7.39×10^5
8	221nm	213nm	1	40.98	11.1×10^5
9	280nm	279nm	1	42.51	12.3×10^5
10	270nm	266nm	4	17.56	13.2×10^5
11	230nm	234nm	4	50.48	4.7×10^5
12	228nm	271nm	43	55.20	8.4×10^5
13	225nm	225nm	0	52.25	6.9×10^5
14	225nm	224nm	1	47.43	7.06×10^5
15	222nm	273nm	51	42.16	2.58×10^5
16	223nm	271nm	48	26.79	12.5×10^5
17	289nm	288nm	1	36.71	13.6×10^5
18	280nm	279nm	1	42.51	14.7×10^5
19	228nm	229nm	1	55.13	9.5×10^{56}
20	269nm	262nm	7	33.18	4.5×10^5
21	232nm	234nm	2	44.83	2.0×10^5
22	254nm	255nm	1	14.34	3.3×10^5

K_b M^{-1}: Binding constants.
[a] % Hypochromicity (H %) = $[A_f - A_b)/A_f] \times 100$, where A_f and A_b represent the absorbance of free and bound compounds.

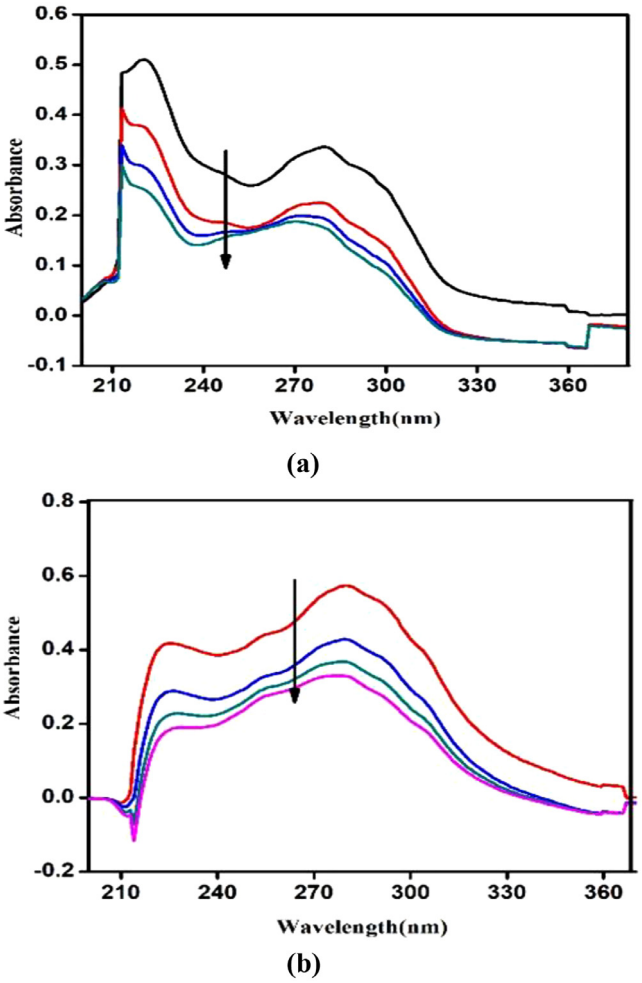

Fig. 3. DNA binding spectra of the compounds (a) **8** and (b) **18**.

imum DNA binding constants were shown by two series of these compounds *i.e.* A (**8, 9** & **10**) and B (**16, 17** & **18**). The binding constants were 11.1 × 10^5 M^{-1}, 12.3 × 10^5 M^{-1} and 13.2 × 10^5 M^{-1} for **8, 9** and **10** and 12.5 × 10^5 M^{-1}, 13.6 × 10^5 M^{-1} and 14.7 × 10^5 M^{-1} for **16, 17** and **18** molecules, respectively. These results confirmed good binding characteristics of the Schiff's bases with DNA. It was observed that the maximum bindings were shown by the molecules having fluorine atoms at benzene rings with different positions. The regression analysis was carried out using Origin software for DNA binding studies. The correlation coefficients (R^2) were in the range of 0.99875-0.99996. The values of regression coefficients were close to one representing the precision of the experiments. Of course, the scales of the DNA binding constants are fairly high, which showed that Schiff's bases may be active against various cancer; through DNA bindings. The different values of DNA binding constants are due to the different polarities of Schiff's bases and configuration. Furthermore, high values of binding constants may be due to the presence of aromatic molecules having heteroatoms in Schiff's bases; as these heteroatoms have good tendency of interactions with DNA [71]. These results clearly indicated that Schiff's bases work through DNA binding on various type of cancer.

2.3. Anticancer study

The synthesized molecules were screened for their anticancer activities with two lung cancer cell lines. The cells used were A549 and H-1229. The various concentrations of the compounds tested were 50, 100, 200, 300 and 400 µg/mL. The anticancer profiles of these compounds are recorded in terms of percentage viabilities (Table 4). The anticancer activities were calculated in terms of percentages. Firstly, the molecules were dissolved in 0.1 % DMSO and the cells with DMSO were applied as vehicle controller. Then, deposit of the molecules was overdue till the control cells touched at lethargic phase. The cells were computed after 24 h. For these compounds, the spread halt for the cells was amplified with emergent concentrations of the compounds. The results showed the important restraint in cancer cell proliferations. The order of the anticancer activities was 50 < 100 < 200 < 300 < 400 µg/mL. The

Table 4
Anticancer activities of the reported molecules with A549 and H1299 lung cancer cell lines.

Compd. No	Percent activities					
	50 µg/mL	100 µg/mL	200 µg/mL	300 µg/mL	400 µg/mL	Control
3	22 (18)	26 (23)	31 (29)	48 (45)	68 (63)	0 (0)
4	32 (30)	39 (37)	41 (40)	54 (56)	64 (72)	0 (0)
5	25 (25)	31 (31)	43 (43)	57 (57)	76 (76)	0 (0)
6	32 (30)	37 (38)	48 (46)	61 (61)	78 (78)	0 (0)
7	24 (28)	31 (35)	39 (43)	51 (55)	67 (71)	0 (0)
8	12 (14)	26 (27)	34 (34)	43 (42)	66 (63)	0 (0)
9	32 (23)	41 (32)	44 (45)	52 (51)	67 (65)	0 (0)
10	29 (32)	37 (40)	46 (49)	52 (55)	72 (76)	0 (0)
11	20 (15)	23 (19)	31 (26)	38 (40)	58 (56)	0 (0)
12	09 (16)	21 (21)	28 (36)	38 (40)	58 (70)	0 (0)
13	31 (22)	42 (32)	45 (40)	51 (45)	69 (68)	0 (0)
14	30 (23)	39 (34)	44 (39)	53 (48)	70 (65)	0 (0)
15	27 (30)	34 (37)	37 (41)	53 (57)	71 (73)	0 (0)
16	20 (15)	25 (20)	38 (33)	44 (39)	69 (63)	0 (0)
17	22 (12)	25 (23)	39 (35)	44 (41)	70 (65)	0 (0)
18	31 (34)	44 (40)	42 (47)	56 (61)	72 (76)	0 (0)
19	26 (30)	35 (39)	40 (44)	52 (56)	67 (71)	0 (0)
20	13 (09)	23 (19)	34 (30)	41 (36)	63 (58)	0 (0)
21	37 (31)	47 (42)	54 (49)	59 (54)	80 (75)	0 (0)
22	39 (36)	43 (47)	52 (54)	59 (59)	76 (78)	0 (0)

The values outside and inside of in parenthesis are of A549 and (b): H1299 lung cancer cell lines.

decree of the anticancer activities was observed at 400 µg/mL and it was in the order of 11 (58) = 12 (58) < 20 (63) < 4 (64) < 8 (66) < 7 (67) = 9 (67) = 19 (67) < 3 (68) < 13 (69) = 16 (69) < 14 (70) = 17 (70) < 15 (71) < 10 (72) 18 = (72) < 5 (76) = 22 (76) < 6 (78) < 21 (80) with A549 cell line. It is clear that the maximum anticancer activities were shown by compounds **5, 6, 21** and **22**; with maximum 80% anticancer activities of compound **21**. The same trend of anticancer activities of these compounds was shown with H-1229 cancer cell line. The order of anticancer activities with this cell line was 11 (56) < 20 (58) < 3 (63) = 8 (63) = 16 (63) < 9 (65) = 14 (65) = 17 (65) < 13 (68) < 12 (70) < 7 (71) = 19 (71) < 4 (72) < 15 (73) < 21 (75) < 5 (76) = 10 (76) = 18 (76) < 6 (78) = 22 (78). It is clear that the maximum anticancer activities were shown by compounds **5, 6, 21 and 22;** with maximum 78% anticancer activities of compound **21**. Slightly higher anticancer activities were observed with A549 than H-1229 cell lines.

A critical evaluation of the structures of these compounds was carried out and it was observed that the molecules **5** and **6** and **21** and **22** are structurally related. Therefore, the molecules **5** and **6** and **21** and **22** have closely related anticancer activities. The anticancer activities of **21** and **22** molecules are greater than **5** and **6** molecules. It is due to the facts that the molecules **21** and **22** have slightly complex structures with more electronegative atoms (10 atoms) than molecules **5** and **6** (6 atoms). Consequently, molecules **21** and **22** interacted slightly stronger with DNA than **5** and **6** molecules; resulting to higher anticancer activities than molecules **5** and **6**. As discussed in Section 3.8 the toxicity of the reported molecules was determined in normal RBC. The reported molecules did not show any toxicity towards the normal cells. The % RSD in all the experiments ranged from 0.86 to 0.95.

2.4. Docking study

The docking studies of the Schiff base compounds with DNA were performed as described in the experimental section. The modeling results of these compounds are given in Table 5. The representative interactions of the two most active compounds of A and B series i.e. **8** and **18** are shown in Fig. 4, while the rest are given in Supplementary information. It is clear from these figures that the Schiff base compounds interacted with DNA differently.

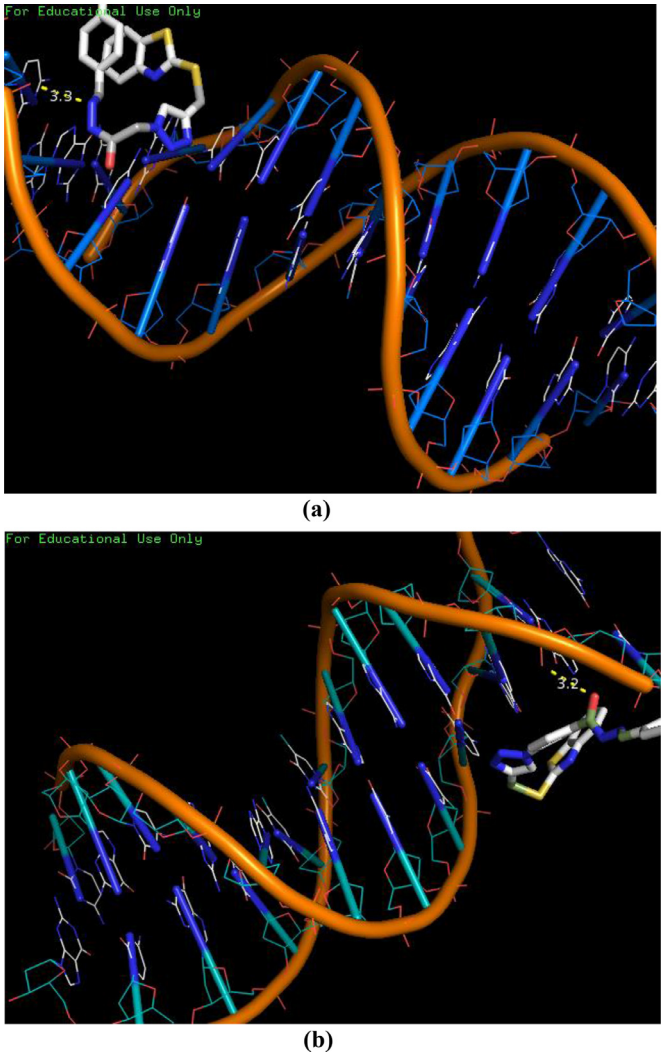

Fig. 4. The docking model of compound (a): **8** and (b): **18** with DNA.

Table 5
Modeling data of the reported compounds.

Compd. No	Binding affinity (kcal mol^{-1})	No. of H bonds	Residues involved in H-bonding (*Bond length in A°*)	Hydrophobic interaction
3	-4.2	1	.263/B/DG'14/O6:: O of -COO- group (3.4)	dc9:: S2 dg10:: C6,C7,S1,C11 dc15::O2,C13,N3,N1 & C7 dg14:: C5,C12,O2,C2 & C4 dt8::N2 & S2
4	-4.8	1	.127/A/DC'9/N4:: N of -N=N-N= group (3.6)	dt8::C14,N2 dc9:: C14&C15 dg10:: C11,C5 & S1 dc15::C3,C6,C17,C16, C12,N1,N5 & C8 dg14:: C4,C10,C17,C8, C2&C1 dc13 :C2
5	-4.3	1	.263/A/DG'10/O6:: N of -N=N-N= group (3.3) .218/B/DG'14/N7:: N of -N=N-N= group (3.4)	dt8::N1&C2 dc9:: C4,&C2 dg10:: C10 & S2 dc15::C11,N3,S2 & C9 dg14:: S2
6	-4.8	1	.624/B/DC'15/OP2:: H of -CONHNH$_2$ group (3.4)	dc9:: C13 & C16 dg10:: C12 &C9 dc15:: C11,C8,C4, C6, C15& C18 dg14:: C1,C2,C9 & N3 dc13::C1 & C2
7	-4.3	1	.263/A/DG'10/O6:: N of -N=N-N= group (3.3) .218/B/DG'14/N7::N of -N=N-N= group (3.4)	dt8:: N1&N3 dc13:: C8,C1,C2&C3 dc15:: C17,N2 & O dg14:: C3,C7&C2 O6 ::C11,C7&N6
8	-4.3	1	.624/B/DG'14/OP2::N of -C=N- group (3.3)	dt8:: C11,C10 & S1 dc9:: C13&C7 dg10:: C13,C14 &C12 dc15:: C7,C14,C8 & C3 dg14:: C18 & C3 dc13::N2
9	-4.8	1	.624/B/DG'14/OP2::O of -CONH- group (3.3) .624/B/DG'14/OP2::N of -N=N-N= group (3.4)	dt8::C2 dg10:: C8&C14 dc15::C9 & C16 dg14:: C19 & N3 dc13::N3 dc9 ::C2,C5,C1&C4 N4 ::C9&C16
10	-5.2	1	.263/A/DG'10/O6::N of -C=N- group (3.3)	dt8::O,N5&C13 dg14:: C7,C6,C2&C16 dc15::N4,C8 & C18 dc13::C1&C2 dc9 ::C18&C13 O6 ::C6,N6&C10 dg16 ::C18
11	-4.7	1	.263/A/DG'10/O6:: N of -C=N- group (3.4)	dt8:: C7 dg16:: C20 dg10:: C14,C18 dg14:: C18,C19 & N4 dc15::C11 & C16 N4 ::C16&C18
12	-4.6	1	.263/A/DG'10/O6:: N of -C=N- group (3.4)	dt8::N6 dg14:: C1,C4,C5,C9,C15, C16&C18 dc15::C7,C5,C3,C14 & C1 dc9 ::C13 dg16 ::C7 dg10 ::C12,C14&C18
13	-4.4	1	.127/A/DC'9/N4:: N of -C=N- group (3.4)	dt8::C10,C11 & N6 dc9:: C7 dg10:: C13,C12 &C14 dc15:: C4,C2,C17,C11, C7&C14 dg14:: C19, C18 & N4 dg16::C7

(*continued on next page*)

Table 5 (*continued*)

Compd. No	Binding affinity (kcal mol^{-1})	No. of H bonds	Residues involved in H-bonding (*Bond length in A°*)	Hydrophobic interaction
14	-4.7	1	.127/A/DC'9/N4:: N of -N=N-N= group (3.3)	dt8:: C11, C10,C16,S1 & N6 dg10:: C13,C15&C19 dc15:: C7,C9&C15 dg16:: C7 dc9 ::C14 dc13 ::N2 dg14 ::C19,C4&C9
15	-4.8	1	.127/A/DC'9/N4:: N of -N=N-N= group (3.5)	dt8:: C18 dc9:: C19,N3&N1 dg10:: C17,C5 & C2 dc15:: C9,C20,S2,N6,C22, C2,C1&C7 dg14:: C2, C9, C6 & C10 dg10::C9 dc13 ::C21,O,N4,N2&C24
16	-5.2	1	.624/B/DC'15/OP2:: O of -CO- group (3.3)	dt8:: C14 dc13::C7,C15,C19,S1,C16 ,C8,N6,C9,C19,C6,C1, C2,C9,C11&C6 dg14:: C24 dc15:: C5,C20,C12,C23, C14&C10 dg14:: C24
17	-5.3	1	.127/A/DC'9/N4:: N of -N=N-N= group (3.5)	dt8:: C17 dc9:: N3, N1 & C18 dg10:: C7&C15 dc15::S2,C19,C7,N6,C21, C2,C5 & C4 dg14:: C7,C4,C2&C8 dc13 ::N2,N4,C24,O,C20
18	-5.5	1	.624/B/DC'15/OP2:: O of -CONH- group (3.2)	dt8:: C17&N3 dc9:: C17 & N1 dg10:: C6C13&sC1 dc15::C15,C18,C19,C24, N5&N1 dg14:: C1,C2,C4&O dc13 ::C2
19	-4.5	1	.127/A/DC'9/N4:: N of -N=N-N= group (3.5)	dt8:: C1&C7 dc9:: C1 dc15::C23,C12&C4 dc13 ::C11,C3,C2,C8,C13,C16,C20, C15,C9,N5,C10&N6
20	-4.9	1	.218/B/DG'14/N7:: O of -CONH- group (3.3) .263/A/DG'10/O6:: O of -CONH- group (3.5)	dc15::C5,C13,C4,C12&C22 dc13 ::C14,N6,C17,C8C11,C3,C2, C16,C20,C9,N5,C10&N5 dg14 ::O1
21	-4.8	1	.127/A/DC'9/N4:: N of -N=N-N= group (3.6)	dt8:: C18 dc9:: C19 & N1 dg10:: C9&C16 dc15::C1,C2,C9,C20&C23 dg14:: C1,C2,C6,C10&C9 dc13 ::C21,N4,N2,C24&O2
22	-4.6	1	.624/B/DG'14/OP2 ::H of -CONH- group(3.5)	dc15::C3,C4,C11&C13 dc13::C9,C21,C16,C8,N6,C17,C7,C14, C10,C1,C2,C10&S1 dg14 ::C22&C4

The hydrogen bonds formed was one in all the molecules. Besides, hydrophobic interactions were also different in different structures. The common hydrophobic residues involved in interaction are dt8, dc9, dc13, dc15, dg15, dg10, dg16 and dg14. The number of hydrogen bonds and the residues of compounds and DNA involved in hydrogen bondings are given in Tables 3. The binding energies of the Schiff base compounds with DNA ranged from -4.2 to -5.5 kcal/mol. These results clearly confirmed the anticancer profiles of the two series of the compounds i.e. A and B with maximum binding energies i.e. -4.3, -4.8 & -5.2 for **8, 9** and **10** and -5.2, -5.3 & -5.5 for **16, 17** and **18** kcal/mole, respectively. Briefly, it is interesting to note that the results of modeling with DNA are supporting the results of anticancer activities. It means that the compounds are working as anticancer molecules through DNA binding. Therefore, the mechanism of the interactions of these molecules is based on DNA interactions through various bonds as discussed above in this section.

3. Experimental

3.1. Chemicals and reagent

The syntheses were carried out using reagents and solvents of the highest quality of analytical reagent grade and were used without further purification. Fine chemicals including 2-mercaptobenzothiazole, ethyl 4-azidobenzoate, 2,4-difluorbenzaldehyde, 2,5-difluorobenzaldehyde, 3,4-difluorobenzal dehyde, 2-hydroxybenzaldehyde, 3-hydroxybenzaldehyde and 4-methoxybenzaldehyde were purchased from BDH Chemicals Ltd., UK. The other fine chemicals used were ethyl azidoacetate,

4-fluorobenzaldehyde, 2-fluoro-3-trifluoromethyl-benzaldehyde sodium methoxide, propargyl bromide (80 wt % in toluene), $CuSO_4$ and Na-ascorbate (Sigma-Aldrich, USA). The solvents used were methanol, ethanol, ethyl acetate, hexane, DMF and DMSO were purchased from Sigma-Aldrich, USA. Calf thymus DNA for DNA binding study was supplied by S.D. Fine Chemicals, Ltd., New Delhi, India.

3.2. Instruments used

All the reactions were monitored by TLC using hexane-ethyl acetate (1:1) mobile phase, which was performed on UV fluorescent Silica gel Merck 60 F254 plates, and the spots were visualized using a UV lamp (254 nm). The measurements of the melting points were performed on a Stuart Scientific SMP1 and are uncorrected. All synthesized compounds were fully characterized by ^{1}H and ^{13}C NMR, IR and Mass analysis. The functional groups were identified using SHIMADZU FTIR-Affinity-1S spectrometer in the range of 400–4000 cm^{-1}. The ^{1}H NMR (400 MHz), ^{13}C NMR (100 MHz) and ^{19}F NMR (376 MHz) spectra were investigated with a Bruker spectrometer (400 MHz) with TMS as internal standard to calibrate the chemical shifts (δ) reported in ppm. The ESI mass spectral data were recorded on MALDI microflex mass spectrometer. UV-Vis spectra for DNA binding were obtained on a T80 UV/VIS Spectrometer (PG Instruments Ltd.). Dulbecco's modified Eagle's medium (DMEM) and antibiotics/antimycotics were supplied by GIBCO NY, USA. The bovine fetal serum (FBS) was bought from HyClone, Utah, USA. Other equipment used were sonicator, centrifuge machine and weighing balance, water bath, biosafety cabinet class 2, laminar airflow, CO_2 incubator, Elisa plate reader and microscope fitted with camera. The ELISA plate reader used for detection of LDH released from the cells at a wavelength of 490 nm, was purchased from Thermo, Multiskan^{TM} FC, (The United States of America).

3.3. General click procedure for the synthesis of ester based-1,2,3-triazoles **3** and **4**

An alkyne **2** (1 mmol) was dissolved in DMSO (10 mL) then treated with a solution of copper sulfate (0.6 mmol, 0.10 g) and sodium ascorbate (0.75 mmol, 0.15 g) in water (10 mL). Thereafter, ethyl azidoacetate and/or ethyl 4-azidobenzoate (1 mmol) was added drop wise with the continued stirring for 6 h at room temperature. After the completion of the reaction; as showed by TLC (hexane-ethyl acetate, 1:1), the reaction was quenched to iced-water furnishing on the formation of a precipitate, which was collected by filtration, then washed with saturated solution of ammonium chloride. The targeted 1,2,3-triazoles **3** and **4** were purified by recrystallization from ethanol/DMF.

3.4. General hydrazinolysis procedure for the synthesis of acid hydrazides **5** and **6**

The desired acid hydrazides **5** and **6** were prepared by refluxing a mixture of ester based-1,2,3-triazole **3** and/or **4** (10 mmol) and hydrazine hydrate (15 mmol) in ethanol (30 ml) for 4 h. The excess of ethanol was then removed; the product separated was collected and purified by recrystallization from ethanol.

3.5. General procedure for the synthesis of Schiff bases **7-22**

An equimolar mixture of hydrazide **5** and/or **6** (1 mmol) and the appropriate benzaldehyde (1 mmol) were dissolved in ethanol (20 ml) and heated under reflux for 6-8 h in the presence of few drops of acetic acid. After cooling, the resulting Schiff bases **7-22** were filtered off and recrystallized from ethanol.

3.6. DNA binding study

DNA binding study is one of the noteworthy gears to judge the activities of the new manufactured molecules. It is because of the fact that the cancer is straight forwardly related with DNA replication. The reported compounds interactions were considered with Ct-DNA (at pH 7.4) in a solution of water including tris-(hydroxymethyl)-amino methane buffer (Tris, 10^{-2} M). Initially, the amount of a fresh prepared Ct-DNA solution was dogged on UV-Vis absorption spectrometer with 260 nm wavelength (ε = 6600 $M^{-1}cm^{-1}$) by expressive its absorbance [72]. The absorption spectra of the reported compounds at fixed amount of (1.6×10^{-4} M) were recorded following with the dissimilar amounts of DNA (1.5×10^{-5}, 1.3×10^{-5} and 1.1×10^{-5}) used. The λ_{max} was noted and the absorbance of the mixture *i.e.* with each unlike solution of DNA and the compounds was also dignified. To produce the constant results, the trials were repeated five times (n = 5). The inherent DNA binding coefficients (K_b) were resolved by Benssi-Hilderbrand equation (Eq. 1) as by Wolfe et *al.* [70]. The Eq. 1 is as follows:

$$[DNA]/(\varepsilon_a - \varepsilon_f) = [DNA]/(\varepsilon_a - \varepsilon_f) + 1/K(\varepsilon_b - \varepsilon_f) \quad (1)$$

Where, absorption coefficients, ε_a, ε_f, and ε_b represents A_{obs}/[compound], extinction coefficient for the complex and the extinction coefficient for the complex in the completely bound form. The inherent binding coefficients for the unlike compounds (K_b) were determined by the separation of slopes and the intercepts of the plots of *[DNA]* / (ε_a - ε_f) *vs [DNA]*.

3.7. Anticancer study

The anti-proliferative vexing of the compounds was finalized with 2 lung cancer cell lines (A549 and H-1229). These cells were sowed in a 96 well plate and incubated. At around 61-71% confluence, the cells were canned with amount of 400, 300, 200, 100, and 50 µg/mL of the reported compounds and allowable to incubate for next 24 h. The cells were inspected by adding 15.0 μL (5.0 mg/mL MTT). At 37°C for 4 h, the separate media from each well were marked. The cells were re-suspended in 100 μL of DMSO and the plate directly covered with aluminum foil, followed by mild shaking on a shaker for around 15 min. Absorbance was noted at 540 nm and the percent halt in proliferation was proposed by the formula in (Eq. 2).

$$\%\,\text{Inhibitaion} = \left[\left(A_{Control} - A_{Sample}\right)/A_{Control}\right] \times 100 \quad (2)$$

3.8. Docking study

The docking studies of 1,2,3-triazole complexes were done by Intel® dual CPU (1.86 GHz) with Windows XP operating system. Marwin Sketch software was utilized to draw the structures of Schiff bases (hydrazones) tethering benzothiazole-1,2,3-triazole conjugates. The structures were cleaned to 3D and saved in PDB file format [73]. After that, the structure of DNA (pdb ID: 1bna) was downloaded from protein data bank. Using AutoDock Tools (ADT) 4.2 the structure of DNA to be docked was prepared by assigning Gastegier charges, merging non-polar hydrogen atoms and saving it in PDBQT file format. Docking was performed with AutoDock 4.2 (Scripps Research Institute, USA) considering all the rotatable bonds of the ligand as rotatable and the receptor as rigid [74]. Using same tool, Schiff bases (hydrazones) tethering benzothiazole-1,2,3-triazole conjugates (as a ligand) were edited to be saved in PDBQT formate. The grid box size of 60 × 80 × 110 A° with 0.375 A° spacing was used. After saving both files in PDBQT formate, Vina software was used to get binding energy/affinity between receptor (DNA) and ligand [Schiff bases]. After using Vina software, the output file was opened in PyMOL to carry out the molecular docking,

virtual screening and binding site analysis and to get an image of interaction and the bond length of hydrogen bond between DNA and Schiff bases tethering benzothiazole-1,2,3-triazole conjugates.

3.9. Hemolysis profiles

The experiments were also carried out for the hemolytic assays of the reported molecules in an adjustment of ASTM standard F-756-00 [71]; based on colorimetric detection of Drabkin's solution. 1.5 mL reported molecules were incubated in 0.215 mL of dilute blood (0.1 mL rabbit blood mixed with 0.9 mL PBS) at 35°C for 4 h. Collected hemoglobin of rabbit blood was observed to be less than 210 μg/mL (basal level for hemolytic test), endorsing the fresh rabbit blood use in test. The solution was centrifuged at 4400 rpm for 25.0 min. To determine the supernatant hemoglobin, 1.5 mL of Drabkin's solution was added to 0.5 mL of supernatant and the sample was permitted to stand for 20 min. The quantity of cyanmethemoglobin in supernatant was estimated at 540 nm and compared with the standard plot (hemoglobin concentrations ranging from 31 to 1062 mg/mL). The percentage hemolysis referred to the ratio of hemoglobin quantities in the supernatant of blood samples not treated and treated with the reported molecules. Also, the absorption of the reported molecules was performed at 540 nm to establish the effect of the absorption of the reported molecules. Finally, saline solution and double distilled water were utilized as negative and positive controls, respectively

4. Conclusion

Encouraged by our reported results, we have attempted on the synthesis of novel macromolecules encompassing benzothiazole-1,2,3-triazole hybrids bearing hydrazone linkage. The structures of newly synthesized hybrid molecules were investigated by several spectroscopic tools as well as the DFT study. The synthesized compounds were analyzed for anticancer activities with A549 and H1299 lung cancer cell lines. The anticancer activities ranged from 55 to 90%. DNA binding study was also carried out to see the mechanism of action and the DNA binding constants were of good value ranging from of 2.0×10^5 and 14.7×10^5 M^{-1}; indicating good interactions of the reported molecules with DNA. Finally, the modeling was confirmed and it was found that the results of modeling were in good agreement with the results of anticancer and DNA binding studies. All these finding confirmed that the reported molecules work as anticancer agents by interacting with DNA. During the discussion it was realized that only those molecules were active having fluorine atoms attached with benzene ring. Therefore, two series of the compounds were identified i.e. **7, 8** & **9** and **16, 17** & **18**. These were quite good active as anticancer drugs.

Credit author statement

Mohamed Reda Aouad conceived the main conceptual idea, directed and devised the project, and proof outline Meshal A. Almehmadi and Ateyatallah Aljuhani carried out the experiment part. Imran Ali performed the anticancer screening and DNA binding, modeling simulations. Nadjet Rezki, Ateyatallah Aljuhani and Shaya Yahya Alraqa performed the spectroscopic measurements and characterization, processed the experimental data, and took the lead in drafting the manuscript and contributed to the interpretation of the results. Mohamed Hagar developed the theoretical formalism, performed the DFT calculations and interpreted the numerical simulations. Imran Ali and Mohamed Reda Aouad supervised the writing and editing the final manuscript. All authors provided critical feedback and helped shape the research, analysis and manuscript and contributed to the final version of the manuscript.

Declaration of Competing Interest

The authors declare that they have no known competing financial interests or personal relationships that could have appeared to influence the work reported in this paper.

Supplementary materials

Supplementary material associated with this article can be found, in the online version, at doi:10.1016/j.molstruc.2020.129148.

References

[1] V. Angelova, V. Karabeliov, P.A. Andreeva-Gateva, J. Tchekalarova, Recent developments of hydrazide/hydrazone derivatives and their analogs as anticonvulsant agents in animal models, Drug Dev. Res. 77 (2016) 379–392.
[2] K.T. Tadele, T.W. Tsega, Schiff bases and their metal complexes as potential anticancer candidates: a review of recent works, Anticancer Agents Med. Chem. 19 (15) (2019) 1786–1795.
[3] M.N. Ahamad, K. Iman, M.K. Raza, M. Kumar, A. Ansari, M. Ahmad, M. Shahid, Anticancer properties, apoptosis and catecholase mimic activities of dinuclear cobalt(II) and copper(II) Schiff base complexes, Bioorg. Chem. 95 (2020) 103561–103575.
[4] A.A. Shanty, J. ElizabethPhilip, E.J. Sneha, M.R.P. Kurup, S. Balachandran, P.V. Mohanan, Synthesis, characterization and biological studies of Schiff bases derived from heterocyclic moiety, Bioorg. Chem. 70 (2017) 67–73.
[5] M. Rudrapal, D. Biplab, Chemistry and biological importance of heterocyclic Schiff'sbases, Int. Res. J. Pure Appl. Chem. 3 (3) (2013) 232–249.
[6] J. De., O.C. Brum, T.C.C. França, S.R. LaPlante, J.D.F. Villar, Synthesis and biological activity of hydrazones and derivatives: a review, Mini-Rev. Med. Chem. 20 (5) (2020) 342–368.
[7] A. Hameed, M. Al-Rashida, M. Uroos, S. Abid Ali, K.M. Khan, Schiff bases in medicinal chemistry: a patent review (2010-2015), Expert Opin Ther. Pat. 27 (1) (2017) 63–79.
[8] Ł. Popiołek, Hydrazide-hydrazones as potential antimicrobial agents: overview of the literature since, Med. Chem. Res. 26 (2017) (2010) 287–301.
[9] K.S. Kumar, S. Ganguly, R. Veerasamy, E. De Clercq, Synthesis, antiviral activity and cytotoxicity evaluation of Schiff bases of some 2-phenyl quinazoline-4(3)H-ones, Eur. J. Med. Chem. 45 (11) (2010) 5474–5479.
[10] S. Aggarwal, D. Paliwal, D. Kaushik, G.K. Gupta, A. Kumar, Pyrazole Schiff base hybrids as anti-malarial agents: synthesis, in vitro screening and computational study, Comb. Chem. High Throughput Screen. 21 (3) (2018) 194–203.
[11] A.M. Alafeefy, M.A. Bakht, M.A. Ganaie, M.N. Ansarie, N.N. El-Sayed, A.S. Awaad, Synthesis, analgesic, anti-inflammatory and anti-ulcerogenic activities of certain novel Schiff's bases as fenamateisosteres, Bioorg. Med. Chem. Lett. 25 (2) (2015) 179–183.
[12] R.N. Gacche, D.S. Gond, N.A. Dhole, B.S. Dawane, Coumarin Schiff-bases: as antioxidant and possibly anti-inflammatory agents, J. Enzyme Inhib. Med. Chem. 21 (2) (2006) 157–161.
[13] F.D. Popp, W. Kirsch, Synthesis of potential anticancer agents. V. Schiff bases and related compounds, J. Org. Chem. 26 (10) (1961) 3858–3860.
[14] C.P. Kaushik, J. Sangwan, R. Luxmi, K. Kumar, A. Pahwa, a), Synthetic routes for 1,4-disubstituted 1,2,3-triazoles: a review, Curr. Org. Chem. 23 (8) (2019) 860–900 b) Rani, G. Singh, A. Singh, U. Maqbool, G. Kaur, J. Singh, CuAAC-ensembled 1,2,3-triazole-linked isosteres as pharmacophores in drug discovery: review, RSC Adv., 10 (2020) 5610-5635.
[15] K. Bozorova, J. Zhaoa, H.A. Aisaa, 1,2,3-Triazole-containing hybrids as leads in medicinal chemistry: a recent overview, Bioorg. Med. Chem. 27 (2019) 3511–3531.
[16] F. Friscourt, G.-J. Boons, One-pot three-step synthesis of 1,2,3-triazoles by copper-catalyzed cycloaddition of azides with alkynes formed by a Sonogashira cross-coupling and desilylation, Org. Lett. 12 (21) (2010) 4936–4939.
[17] L. Zhou, A. Amer, M. Korn, R. Burda, J. Balzarini, E. De Clercq, E.R. Kern, P.F. Torrence, Synthesis and antiviral activities of 1,2,3-triazole functionalized thymidines: 1,3-dipolar cycloaddition for efficient regioselective diversity generation, Antivir. Chem. Chemother. 16 (6) (2005) 375–383.
[18] S.K. Avula, A. Khan, N. Ur Rehman, M.U. Anwar, Z. Al-Abri, A. Wadood, M. Riaz, R. Csuk, A. Al-Harrasi, Synthesis of 1*H*-1,2,3-triazole derivatives as new α-glucosidase inhibitors and their molecular docking studies, Bioorg. Chem. 81 (2018) 98–106.
[19] F. Ahmadi, M.R. Ghayahbashi, M. Sharifzadeh, E. Alipoiur, S.N. Ostad, M. Vosooghi, H.R. khademi, M. Amini, Synthesis and evaluation of anti-inflammatory and analgesic activities of new 1,2,4-triazole derivatives, Med. Chem. 11 (1) (2014) 69–76.
[20] S. Wang, H. Liu, X. Wang, K. Lei, G. Li, Z. Quan, Synthesis and evaluation of antidepressant activities of 5-aryl-4,5-dihydrotetrazolo[1,5-*a*]thieno[2,3-*e*]pyridine derivatives, Molecules 24 (10) (2019) 1857.
[21] S.G. Khanage, A. Raju, P.B. Mohite, R.B. Pandhare, Analgesic activity of some 1,2,4-triazole heterocycles clubbed with pyrazole, tetrazole, isoxazole and pyrimidine, Adv. Pharm. Bull. 3 (1) (2013) 13–18.

[22] V. Sumangala, B. Poojary, N. Chidananda, J. Fernandes, N.S. Kumari, Synthesis and antimicrobial activity of 1,2,3-triazoles containing quinoline moiety, Arch. Pharm. Res. 33 (12) (2010) 1911–1918.

[23] T. Gregorić, M. Sedić, P. Grbčić, A.T. Paravić, S.K. Pavelić, M. Cetina, R. Vianello, S. Raić-Malić, Novel pyrimidine-2,4-dione-1,2,3-triazole and furo[2,3-*d*]pyrimidine-2-one-1,2,3-triazole hybrids as potential anti-cancer agents: synthesis, computational and X-ray analysis and biological evaluation, Eur. J. Med. Chem. 125 (2017) 1247–1267.

[24] M.J. Soltis, H.J. Yeh, K.A. Cole, N. Whittaker, R.P. Wersto, E.C. Kohn, Identification and characterization of human metabolites of CAI [5-amino-1-1(40-chlorobenzoyl-3,5-dichlorobenzyl)-1,2,3-triazole-4-carboxamide), Drug Metab. Dispos. 24 (1996) 799–806.

[25] C. Sheng, W. Zhang, New lead structures in antifungal drug discovery, Curr. Med. Chem. 18 (2011) 733–766.

[26] R. Del Busto, E. Haas, T. Madhaven, K. Burch, F. Cox, E. Fisher, E. Quinn, D. Pohlod, *In vitro* and clinical studies of cefatrizine, a new semisynthetic cephalosporin, Antimicrob, Agents Chemother. 9 (1976) 397–405.

[27] N. Rezki, A Green ultrasound synthesis, characterization and antibacterial evaluation of 1,4-disubstituted 1,2,3-triazoles tethering bioactive benzothiazole nucleus, Molecules 21 (2016) 505–517.

[28] N. Rezki, M.R. Aouad, Green ultrasound-assisted three-component click synthesis of novel 1*H*-1,2,3-triazole carrying benzothiazoles and fluorinated-1,2,4-triazole conjugates and their antimicrobial evaluation, Acta Pharm. 67 (2017) 309–324.

[29] M.R. Aouad, M.A. Soliman, M.O. Alharbi, S.K. Bardaweel, P.K. Sahu, A.A. Ali, M. Messali, N. Rezki, Y.A. Al-Soud, Design, synthesis and anticancer screening of novel benzothiazole-piperazine-1,2,3-triazole hybrids, Molecules 23 (2018) 2788–2801.

[30] M.R. Aouad, M.A. Almehmadi, N. Rezki, F.F. Al-blewi, M. Messali, I. Ali, Design, click synthesis, anticancer screening and docking studies of novel benzothiazole-1,2,3-triazoles appended with some bioactive benzofused heterocycles„ J. Mol. Struct. 1188 (2019) 153–164.

[31] T.L. Dadmal, K. Appalanaidu, R.M. Kumbhare, T. Mondal, M.J. Ramaiah, M. Pal Bhadra, Synthesis and biological evaluation of triazole and isoxazole tagged benzothiazole/benzoxazole derivatives as potent cytotoxic agents, New J. Chem. 42 (2018) 15546–15551.

[32] R.M. Kumbharea, T.L. Dadmala, M.J. Ramaiahb, K.S.V. Kishorea, S.N.C.V.L. Pushpa Vallic, S.K. Tiwaric, K. Appalanaidua, Y.K. Raoa, M. Pal Bhadra, Synthesis and anticancer evaluation of novel triazole linked *N*-(pyrimidin-2-yl)benzo[*d*]thiazol-2-amine derivatives as inhibitors of cell survival proteins and inducers of apoptosis in MCF-7 breast cancer cells, Bioorg. Med. Chem. Lett. 25 (2015) 654–658.

[33] N.N. Rao, E. kishan, K. Gopichand, R. Nagaraju, P. Venkateswar Rao, Design, synthesis, spectral characterization, DNA binding, photo cleavage and antibacterial studies of transition metal complexes of benzothiazole Schiff base, Chemical Data Collections 27 (2020) 100368–100380.

[34] R.K. Mohapatra, A.K. Sarangi, M. Azam, M.M. El-ajaily, D.C. Dash, Synthesis, structural investigations, DFT, molecular docking and antifungal studies of transition metal complexes with benzothiazole based Schiff base ligands, J. Mol. Struct. 11795 (2019) 65–75.

[35] M.T. Gabr, N.S. El-Gohary, E.R. El-Bendary, M.M. El-Kerdawy, N. Ni, Synthesis, in vitro antitumor activity and molecular modeling studies of a new series of benzothiazole Schiff bases, Chin. Chem. Lett. 27 (3) (2016) 380–386.

[36] T.B. Shaik, S.M. Ali-Hussaini, V.L. Nayak, M.L. Sucharitha, A. Kamal, Rational design and synthesis of 2-anilinopyridinyl-benzothiazole Schiff bases as antimitotic agents, Bioorg. Med. Chem. Lett. 27 (111) (2017) 2549–2558.

[37] C. Shinu, S. Subir, A novel approach towards design, synthesis and evaluation of some Schiff base analogues of 2-aminopyridine and 2-aminobezothiazole against hepatocellular carcinoma, Biomed. Pharmacoth. 89 (2017) 162–176.

[38] V. Paola, G. Athina, I. Matteo, B. Bernadetta, P. Graziella, C.C. Alba, L.C. Paolo, Synthesis and biological evaluation of benzo[d] isothiazole, benzothiazole and thiazole Schiff bases, Bioorg. Med. Chem. 11 (22) (2003) 4785–4789.

[39] N. Rezki, M.M. Mayaba, F.F. Al-blewi, E.S.H. El Ashry, M.R. Aouad, Click 1,4-regioselective synthesis, characterization, and antimicrobial screening of novel 1,2,3-triazoles tethering fluorinated 1,2,4-triazole and lipophilic side chain, Res. Chem. Intermed. 43 (2017) 995–1011.

[40] N. Rezki, Green microwave synthesis and antimicrobial evaluation of novel triazoles, Org. Prep. Proced. Int. 49 (2017) 525–541.

[41] M.R. Aouad, M.M. Mayaba, A. Naqvi, S.K. Bardaweel, F.F. Al-blewi, M. Messali, N. Rezki, Design, synthesis, *in-silico* and *in-vitro* antimicrobial screenings of novel 1,2,4-triazoles carrying 1,2,3-triazole scaffold with lipophilic side chain tether, Chem. Cent. J. 11 (2017) 117–129.

[42] M.R. Aouad, Click synthesis and antimicrobial screening of novel isatin-1,2,3-triazoles with piperidine, morpholine or piperazine moieties, Org. Prep. Proced. Int. 49 (2017) 216–227.

[43] F.F. Al-blewi, M.A. Almehmadi, M.R. Aouad, S.K. Bardaweel, P.K. Sahu, M. Messali, N. Rezki, E.S.H. El Ashry, Design, synthesis, ADME prediction and pharmacological evaluation of novel benzimidazole-1,2,3-triazole-sulfonamide hybrids as antimicrobial and antiproliferative agents, Chem. Cent. J. 12 (2018) 110–123.

[44] I. Ali, Nano anti-cancer drugs: pros and cons and future perspectives, Curr. Cancer Drug Targets 11 (2011) 131–134.

[45] I. Ali, M.N. Lone, Z.A. Al-Othman, A. Al-Warthan, Heterocyclic scaffolds: centrality in anticancer drug development, Curr. Drug Target 16 (2015) 711–734.

[46] I. Ali, H.Y. Aboul-Enein, A. Ghanem, Enantioselective toxicities and carcinogenesis, Curr. Pharmceut. Anal. 1 (2005) 109–125.

[47] I. Ali, K. Rahis-ud-din, H.Y. Saleem, A. Aboul-Enein, Rather, social aspects of cancer genesis, Can. Ther. 8 (2011) 6–14.

[48] I. Ali, M.N. Lone, H.Y. Aboul-Enein, Imidazoles as potential anticancer agents, Med. Chem. Commun. 8 (2017) 1742–1773.

[49] I. Ali, W.A. Wani, K. Saleem, A. Haque, Thalidomide: a banned drug resurged into future anticancer drug, Curr. Drug Ther. 7 (2012) 13–23.

[50] B.G.M. Youssif, S.G. Abdel-Moty, I.M. Sayed, Synthesis and biological evaluation of some novel 1,2,3-triazol-n-arylidene acetohydrazide incorporating benzimidazole ring moiety as potential antimicrobial agents, J. Curr. Chem. Pharm. Sc. 4 (2014) 54–64.

[51] M.R. Aouad, M. Messali, N. Rezki, A.A. Ali, A. Lesimple, Synthesis and characterization of some novel 1,2,4-triazoles, 1,3,4-thiadiazoles and Schiff bases incorporating imidazole moiety as potential antimicrobial agents, Acta Pharmaceutica 65 (2015) 117–132.

[52] N. Rezki, S.A. Al-Sodies, M.R. Aouad, S. Bardaweel, M. Messali, E.S.H. El Ashry, An eco-friendly ultrasound-assisted synthesis of novel fluorinated pyridinium salts-based hydrazones and antimicrobial and antitumor screening, Int. J. Mol. Sci. 17 (2016) 766–785.

[53] V.A. D'yakonov, E.S. Finkelshtein, A.G. Ibragimov, Dzhemilev reaction for the synthesis of spiro [3.3] heptane and spiro [3.4] octanes, Tetrahedron Lett. 48 (49) (2007) 8583–8586.

[54] P. Kumar, K. Kadyan, M. Duhan, J. Sindhu, V. Singh, B.S. Saharan, Design, synthesis, conformational and molecular docking study of some novel acyl hydrazone based molecular hybrids as antimalarial and antimicrobial agents, Chem. Cent. J. 11 (2017) 115–128.

[55] P. Patorski, E. Wyrzykiewicz, G. Bartkowiak, Synthesis and conformational assignment of *n*-(e)-stilbenyloxymethylenecarbonyl-substituted hydrazones of acetone and *o*-(*m*- and *p*-) chloro- (nitro-) benzaldehydes by means of ^{1}H and ^{13}C NMR Spectroscopy, J. Spectr. (2013) (2013) 1–12.

[56] E. Wyrzykiewicz, D. Prukaʒä, New isomeric *N*-substituted hydrazones of 2-, 3- and 4-pyridinecarboxaldehydes, J. Heter. Chem. 35 (1998) 381–387.

[57] G. Palla, G. Predieri, P. Domiano, C. Vignali, W. Turner, Conformational behaviour and E/Z isomerization of N-acyl and N-aroylhydrazones, Tetrahedron 42 (13) (1986) 3649–3654.

[58] M. Hagar, S.M. Soliman, F. Ibid, E.S.H. El Ashry, Quinazolin-4-yl-sulfanylacetyl-hydrazone derivatives; synthesis, molecular structure and electronic properties, J. Mol. Struct. 1049 (2013) 177–188.

[59] I. Litvinov, O. Kataeva, L. Ermolaeva, G. Vagina, T. Troepol'skaya, V. Naumov, Crystal and molecular structure of aroyl-and acetylhydrazones of acet-and benzaldehydes, Bulletin of the Academy of Sciences of the USSR, Div. Chem. Sci. 40 (1) (1991) 62–67.

[60] I. Ali, K. Saleem, D. Wesselinova, A. Haque, Synthesis, DNA binding, hemolytic and anticancer assays of curcumin I based ligands and their ruthenium (III) complexes, Med. Chem. Res. 22 (2013) 1386–1398.

[61] I. Ali, W.A. Wani, K. Saleem, M.F. Hseih, Design and synthesis of thalidomide based dithiocarbamate Cu(II), Ni(II) and Ru(III) complexes as anticancer agents, Polyhedron 56 (2013) 134–143.

[62] K. Saleem, W.A. Wani, A. Haque, M.N. Lone, M.F. Hsieh, M.A. Jairajpuri, I. Ali, Synthesis, DNA binding, hemolysis assays and anticancer studies of copper(II), nickel(II) and iron(III) complexes of a pyrazoline based ligand, Future Med. Chem. 5 (2013) 135–146.

[63] I. Ali, W.A. Wani, K. Saleem, D. Wesselinova, Syntheses, DNA binding and anticancer profiles of *L*-Glutamic acid ligand and it's copper(II) and ruthenium(III) complexes, Med. Chem. 9 (2013) 11–21.

[64] I. Ali, W.A. Wani, K. Saleem, M.F. Hsieh, Anticancer metallodrugs of glutamic acid sulphonamides: *in silico*, DNA binding, hemolysis, and anticancer studies, RSC Adv. 4 (2014) 29629–29641.

[65] R.E. Smith, Drugs that Act on DNA or RNA, In Medicinal Chemistry - Fusion of Traditional and Western Medicine (2013) 329–335 V1.

[66] I. Ali, M.N. Lone, Z.A. Al-Othman, A. Alwarthan, Insights into the pharmacology of new heterocycles embedded with oxopyrrolidine rings: DNA binding, molecular docking, and anticancer studies, J. Mol. Liq. 234 (2017) 391–402.

[67] N. Kumar, N. Lal, V. Nemaysh, P.M. Luthra, Design, synthesis, DNA binding studies and evaluation of anticancer potential of novel substituted biscarbazole derivatives against human glioma U87 MG cell line, Bioorg. Chem. 100 (2020) 103911.

[68] M.E. Reichmann, S.A. Rice, C.A. Thomas, P. Doty, A further examination of the molecular weight and size of desoxypentose nucleic acid, J. Am. Chem. Soc. 76 (1954) 3047–3053.

[69] G. Pratviel, J. Bernadou, B. Meunier, DNA and RNA cleavage by metal complexes, Adv. Inorg. Chem. 45 (1998) 251–312.

[70] A. Wolfe, G.H. Shimer, T. Meehan, Polycyclic aromatic hydrocarbons physically intercalate into duplex regions of denatured DNA, Biochem. 26 (1987) 6392–6396.

[71] M. Evstigneev, DNA-binding aromatic drug molecules: physico-chemical interactions and their biological roles, Lap Lambert Academic Publishing 2001.

[72] G.M. Morris, D.S. Goodsell, R.S. Halliday, R. Huey, W.E. Hart, R.K. Belew, A.J. Olson, Automated docking using a lamarckian genetic algorithm and empirical binding free energy function, J. Comput. Chem. 19 (1998) 1639–1662.

[73] N. Ataci, E. Ozcelik, N. Arsu, Spectrophotometric study on binding of 2-thioxanthone acetic acid with ct-DNA, Spectrochim, Acta Part A 204 (2018) 281–286.

[74] M.F. Sanner, Python: a programming language for software integration and development, J. Mol. Graph. Model. 17 (1999) 57–61.